NASA Technical Memorandum 83148

MISSION LOAD DYNAMIC TESTS OF TWO UNDENSIFIED SPACE SHUTTLE THERMAL PROTECTION SYSTEM TILES

JACK D. LEATHERWOOD AND JOE C. GOWDEY

JUNE 1981

National Aeronautics and
Space Administration

Langley Research Center
Hampton, Virginia 23665

SUMMARY

Two tests of undensified Space Shuttle thermal protection tiles under combined static and dynamic loads have been conducted. The tiles had a density of approximately 144 Kg/m^3 (LI900 tiles) and were mounted on a strain isolation pad which was 0.41 cm (.160 inch) thick. A combined static and dynamic mission stress histogram representative of the W-3 area of the wing of the orbiter vehicle was applied. The stress histogram was provided by the Space Shuttle Project. Results presented in this paper include: tabulation of measured peak and root-mean-square (RMS) accelerations in both compression and tension; peak SIP stress in compression and tension, peak and RMS amplitude response ratios; lateral to vertical response ratios; response time histories; peak stress distributions (histograms), and SIP extension measured both with and without static tension at various mission times.

INTRODUCTION

The Space Shuttle contains in excess of 30,000 ceramic tiles for protection of the aluminum substructure from the high temperature of reentry. These tiles are attached to the Shuttle by first bonding each tile to a felt material called Strain Isolator Pad (SIP) and then bonding the combination to the substructure. The configuration defined by the tile-adhesive-SIP represents a complex system that exhibits unique response to static and dynamic loading. The structural mechanics properties of the tile/SIP system have been under investigation at NASA Langley Research Center (LaRC) with a particular emphasis upon developing a data base for the assessment and/or prediction of tile fatigue life.

Several studies (see refs. 1-3, for example) have characterized the nonlinear stress-strain behavior of the SIP material and defined static failure modes and loads for both densified and undensified tiles. This nonlinear relationship between the tile load and tile displacement results in a complex nonlinear response behavior as discussed in reference 4. For example, large stress amplifications due to sharp peaks in tile acceleration response waveform were observed and parametric response under certain sinusoidal excitations occurred. Other studies (ref. 5, for example) have investigated fatigue properties of the tile/SIP system under constant amplitude, fully reversed sinusoidal loading applied at a frequency of 1 hertz. The results of these tests, however, do not reflect the effect of nonsinusoidal, high strain rate response of the tiles such as would actually be experienced in flight. It is the purpose of this paper to present and summarize the results of an experimental investigation to obtain dynamic response data under high strain rate conditions for use in assessment of tile dynamic response and fatigue life.

Two high stress level tests of LI 900/.160 (tile type/SIP thickness in inches) undensified tiles representative of the W-3 area of the orbiter vehicle were conducted. In these tests, the tiles were subjected to static tensile stress combined with a dynamic stress histogram corresponding to an expected mission load profile. The mission load histogram was applied repeatedly until tile failure occurred or until 1500 simulated missions were achieved. The magnitude of the applied loads were provided by the Project. In this paper, the rationale used to develop the test loads is not discussed. Further, no attempt is made to interpret the data in terms of fatigue properties or fatigue life of the Thermal Protection System (TPS). Details of the test configurations, procedures, and limitations are discussed, since they can influence the interpretation of the results obtained. In particular, some of the practical problems that arose because of the system nonlinear response characteristics are noted.

Test Specimens

Two specimens were tested, both of which were LI900 undensified tiles having footpad dimensions of 15.24 x 15.24 cm (6" x 6") but different thicknesses (5.1 and 7.0 cm). The tiles were bonded to a 28 x 28 x 1.27 cm (11" x 11" x 0.5") flat aluminum substrate plate with filler bar added. The substrate plate was then bolted to the fixture plate of the vibration shaker. No attempt was made in these tests to simulate substrate deformation.

In order to obtain the required stress levels in the SIP, it was necessary to bind a 15.24 x 15.24 x 0.95 cm (6" x 6" x .375") steel plate (net weight = 1.63 kg (3.6 lbs.)) to the tile upper surface. The center of this steel plate contained an eye bolt for attaching a 1.0 cm (3/8 in.) bungee cord that was used to produce static tensile stress in the SIP. A sketch of the fatigue specimen and test configuration is shown in figure 1. In the remainder of this paper, the two tile/SIP specimens will be referred to as Tile FLD-2 (5.1 cm (2.0") thick) and Tile FLD-4 (7.0 cm (2.75") thick).

Test Apparatus

Vibration system.- An electromagnetic vibration exciter was used to excite the tiles. The exciter is capable of producing 44,482 N (10,000 lbs.) of force at frequencies from 5 to 2500 Hz, within the limitations imposed by the armature mass of 445 kg (110 lbs.) and velocity/displacement limits of 190 cm/sec (75 in/sec), and 2.5 cm (1 in.) double amplitude, respectively. The requirements of this test were sufficiently below the machine capabilities that there were no constraints imposed by the equipment.

Control system.- A digital control system was used to generate the vibration spectrum and control the applied vibration levels. The sine vibration mode of operation was chosen with the frequency selected to be below the natural frequency

of the test specimen but high enough to minimize the time required to apply a discrete number of load cycles to the specimen. A nominal test frequency of 100 Hz was chosen.

A feedback source for the controller was chosen to be a pair of accelerometers mounted on diagonal corners of the tile top, and these were designated the control accelerometers. The controller operates by varying the drive signal to the vibration exciter to maintain the tile acceleration level, as measured by the control accelerometer receiving the higher peak acceleration, at the level specified by the reference spectrum.

Instrumentation.- Four accelerometers were mounted to the steel top plate of the tile, oriented to measure accelerations in the vertical (perpendicular to the plane of the SIP) direction. A diagonal pair of these accelerometers were designated the control accelerometers. Another pair of accelerometers, mounted orthogonally at diagonal corners of the steel plate, measured lateral accelerations. An additional accelerometer measured the input acceleration (vertical) of the vibration exciter fixture plate.

Two noncontacting, nonforce inducing position transducers were placed to obtain vertical displacement information from the tile top. Two position sensors were also located at opposite ends of one side of the tile, sensing lateral motions. A fifth position sensor obtained table motion information in the vertical direction. These noncontacting displacement sensors consist of a variable impedance bridge with an active and a reference coil. The variations in impedance result from the eddy currents induced in nearby conductive surfaces. The conductive target for the vertical sensors was the steel top plate, whereas aluminum tape was added to the side of the tile to provide a lateral conductive target. The effective range of the sensors used was about 2.5 cm (1 in.).

Accuracy is about $\pm$ .003 cm over a range of 1 to 2.5 cm. The locations of the accelerometers and position transducers are shown in figure 1. Also attached to the steel top plate was a bungee cord used to develop static stress in the SIP as required by the stress histogram (see next section). The bungee was, in turn, attached to a load cell and overhead power lift.

Test Procedures

The load cycle histogram of figure 2 was supplied as representative of one mission. In the tests described herein, only the stress bins between 20,685 Pa and 55,160 Pa (3.0 and 8.0 psi) were used. In order to implement the dynamic component of this histogram with the vibration exciter controller, the reference spectrum of figure 3 was developed. This spectrum represents a 10 mission block and contains very close to the exact number of load cycles (multiplied by 10) that would be required by the histogram. The spectrum was swept in frequency because the controller is incapable of changing output level without simultaneously changing frequency. A swept (rather than stepwise) level change was used in order to minimize the effects of the rate-of-change time constant inherent to the controller. For this reason also, the rate of change of level was made as constant as practical.

Because of nonlinear stress-strain behavior of the SIP which results in distorted response waveforms, a slight overtest of Tile FLD-2 occurred due to the nonsinusoidal response of the tile/SIP system. The controller is factory programmed to average the positive and negative peak input received from each control accelerometer and control the exciter to maintain that average at the level specified by the reference spectrum. Since the ratio of the compression to tension response peak varies with stress level, and insufficient data existed to predict what the ratios would be at the various stress levels, the controller

was allowed to maintain the average level of each load cycle for Tile FLD-2. For Tile FLD-4, a signal conditioner was inserted in the accelerometer signal path. The conditioner acted to increase the apparent level of the compression peak to be equal to the tension peak. The controller then accurately applied the desired peak stress spectrum. A block diagram of the signal conditioner is shown in figure 4. Note that the signal conditioner produces a square wave output. Because the controller develops the drive signal based upon the peak value of control accelerometer signal, modification of the waveshape by the signal conditioner did not affect controller performance. A detailed description of the operation and function of the signal conditioner is given in Appendix A.

Method of application.- Prior to each test, the accelerometers were attached to the shaker fixture plate and calibrated by application of a $\pm$ 10 g acceleration level at 44.3 Hz. This produced an easily measured 0.245 cm (0.1 in.) double amplitude displacement. The displacement sensors were calibrated statically using the actual specimens as targets (see Instrumentation Section). The specimens were then mounted to the shaker fixture plate, the bungee cord and accelerometers attached, and the desired tension load was applied by pulling the bungee vertically with an electrically-powered lift. Tension force was monitored by a load cell attached between the bungee and lift. Once the desired tension force was attained, the static extension of the SIP was recorded from a digital readout of the displacement sensor output. The dynamic loading was then applied via the vibration exciter in consecutive groups of 10 mission cycles. At the completion of each set of 50 missions, the test was stopped and SIP extension was recorded with the static tension load still applied. The static load was then removed and SIP extension was recorded for the unloaded

condition. Next, the static load was reapplied and the tests were continued. The above sequence was repeated after every group of 50 missions. The test continued until SIP failure occurred or until 1500 missions were completed. The first test (Tile FLD-2) used a static SIP stress of 22,408 Pa (3.25 PSI), equivalent to 361.42 N (81.25 lbs.) tension force, and the second test (Tile FLD-4) used a SIP stress of 17,237 Pa (2.50 PSI), equivalent to 278 N (62.5 lbs.) tension.

Results and Discussion

Response time histories.- Characteristics of tile response to sinusoidal base (table) excitation at both high and low SIP stress levels are illustrated by the response time histories in figures 5 through 8. Each figure contains the table excitation, tile vertical acceleration response at each accelerometer location, and lateral acceleration response. Accelerometer locations are shown on top view of figure 1. Acceleration response time histories for low and high stress level conditions for Tile FLD-2 are shown in figures 5 and 6, respectively. Figures 7 and 8 present similar data for Tile FLD-4. In both tests, the acceleration response time histories were reasonably sinusoidal in shape at low stress levels. However, as the stress level increased, the tile response characteristics became decidedly nonlinear as evidenced by the sharp negative acceleration (tension) peaks, which in some cases, exceeded twice the magnitude of the corresponding compression peaks (see figs. 8(b) and 8(c), for example). The nonsymmetrical response can be characterized by the ratio of compressive acceleration to tension acceleration. This ratio is presented in figure 9 as a function of peak SIP stress (static + dynamic) level. Data are shown for both tiles and for measurements made early and late in the test sequence. The data for Tile FLD-2 indicate that tile/SIP response was approximately sinusoidal

($G_{comp}/G_{tens} \approx 1.0$) only at the lowest stress levels and became increasingly nonsymmetrical as SIP stress increased. Measurements taken at the end of 700 missions (shaded circles) showed little change in the nonsymmetry characteristic, indicating that the basic dynamic response signature of this tile was unaffected by the load history. This tile failed at 710 missions, which corresponds to more than 10^7 load cycles at greater than 34,475 Pa (5.0 PSI).

The dynamic response time histories for Tile FLD-4 indicated a substantial increase in nonsymmetry as compared to Tile FLD-2. Tile FLD-4 completed 1500 missions. Measurements made just prior to the end of the test showed a shift to a more symmetric response as indicated by the shaded squares in figure 9. Several factors that may account for the difference in response characteristics between the two tiles include: (1) different static loads, hence, different R ratios (see eq. (3)) due to the different applied dynamic stress components; (2) shift in tile resonant frequency due to the different tension loads; and (3) more accurate control of tile response for Tile FLD-4 because of insertion of signal conditioning into the shaker control loop. The reduction in response nonsymmetry for Tile FLD-4 at 1500 missions could have been the result of SIP softening under the higher dynamic stress component and extended mission time.

Response levels.- Peak acceleration responses in compression and tension at each accelerometer location are listed in Tables I and II for various mission times. With regard to the lateral accelerometers, the terms tension and compression refer to the lateral peaks that occurred simultaneously with the vertical tension and compression peaks. The table entries are the peak tension and corresponding compression accelerations measured within the 10 mission group preceding the number of missions listed in the far left column. At each accelerometer location, the peak accelerations were averaged over missions to

give the mission average at the bottom of each column. In addition, at each number of missions, the four vertical tile accelerations were averaged and tabulated in the far right column.

Accelerometer measurements at each location varied only slightly as the number of missions increased. This illustrates the ability of the shaker controller to consistently maintain relatively constant tile acceleration response levels even though SIP characteristics may have changed with repeated loading. Second, the nonsymmetry of tile vertical response is apparent. Finally, peak tile acceleration levels experienced by Tile FLD-2 were greater than those of Tile FLD-4 in both compression and tension because insertion of the signal conditioner in the control loop (see test spectrum discussion) resulted in an effective reduction in table acceleration applied to Tile FLD-4 compared to Tile FLD-2. RMS acceleration levels corresponding to the peak accelerations in Tables I and II are given in Table III. The ratio of mission averaged peak tile acceleration response to mission averaged peak table acceleration are given in Table IV (a) and (b). The data show that the amplification ratio for peak tile acceleration response was approximately 3.0 for both tiles whereas the ratio of RMS tile acceleration to RMS table acceleration was about 1.55 for Tile FLD-2 and 1.72 for Tile FLD-4. For a linear dynamic system, the peak and RMS acceleration ratios are identical. The above differences reflect the effect of the nonlinear SIP characteristics. This nonlinearity is further illustrated in Table V, which presents the ratio of average peak acceleration to average RMS acceleration for each vertical accelerometer. The average values refer to the average over mission time; i.e., the column averages in Tables I (b), II (b), and III (a) and (b). The peak to RMS ratio for Tile FLD-2 was approximately 3.2 and for Tile FLD-4 approximately 2.5 to 2.6. If the SIP were linear, the peak to RMS ratio would be 1.4.

Table VI presents the ratio of average (over mission time) peak lateral acceleration response to the overall averaged (over mission time and location) peak vertical response. The maximum lateral response observed in these tests occurred for Tile FLD-2 and equalled approximately 15 percent of the corresponding vertical response. For Tile FLD-2, the maximum lateral response was 3.3 percent of vertical response. In both cases, the lateral frequency was identical to the vertical frequency, although waveform analysis showed the presence of appreciable amounts of one-half, second, and third harmonics which were not coherent with the tile vertical response waveshape.

SIP stress.- The SIP stress levels were derived from the acceleration measurement by application of the following equations:

$$(\sigma_{SIP})_{TENSION} = \sigma_{STATIC} + \frac{Gt}{K} \tag{1}$$

$$(\sigma_{SIP})_{COMP} = \sigma_{STATIC} - \frac{Gc}{K} \tag{2}$$

where

$(\sigma_{SIP})_{TENSION(COMP)}$ = SIP tensile (compressive) stress assuming uniform stress distribution over the SIP footprint, Pa(lb/in^2)

σ_{STATIC} = Static tensile stress due to bungee pull, Pa(lb/in^2)

Gt = Acceleration in tension direction, g units

Gc = Acceleration in compression direction, g units

K = Ratio of footprint area divided by total tile weight, $m^2/Kg(in^2/lb)$, $K = 8.16 \times 10^{-3}(5.740)$ for FLD-2 and $K = 7.96 \times 10^{-3}(5.594)$ for FLD-4

For both tests, the desired (nominal) maximum SIP stress was 55160 Pa (8.0 PSI). The actual SIP stresses obtained (based upon eqs. (1) and (2)) are given in Table VII. It is seen in Table VII (a) that Tile FLD-2 experienced SIP

stresses in excess of 62055 Pa (9.0 PSI) (average SIP stress = 64675 PA (9.38 PSI)). This overstress condition resulted from strong nonsymmetry in tile response which inadvertantly introduced a larger than desired shaker drive signal at the high stress condition. This overstress condition does not invalidate the data obtained from Tile FLD-2. It will, however, influence predicted fatigue life which must be based upon the actual load experience of an individual tile.

Introduction of the signal conditioner (see test spectrum section) in the feedback control loop resulted in the peak stress levels given in Table VII (b) for Tile FLD-4. The use of the signal conditioner led to a reduction in peak stress by approximately 6895 Pa (1.0 PSI). The average peak stress for the Tile FLD-4 was 57918 Pa (8.4 PSI) compared to 6483 Pa (9.4 PSI) for Tile FLD-2. Also listed in Tables VII (a) and (b) are the average R values at the high stress condition where R is defined as:

$$R = \frac{\sigma_{MAX}}{\sigma_{MIN}} \tag{3}$$

The data probably of most use to fatigue specialists are the actual load experiences of each tile; i.e., the distribution of peak stress occurrences. These data are summarized in Tables VII (a) and (b) and in figures 10 and 11. Each table contains the actual number of peak stress occurrences within a 10-mission block taken early (41-50 missions, column 2) in the test and within a 10-mission block taken late (column 3) in the test. The far right column in each table contains the desired peak stress occurrences and the far left column identifies the stress bins within which the peak stress events occurred. In both tests, the actual peak count slightly exceeded the nominal count. This probably was due to counting of secondary peaks (see figs. 6 and 8,

for example) that were present at the highest stress levels. Further, the peak stress distribution for Tile FLD-2 differed greatly from the nominal distribution, particularly within the higher stress bins. Approximately 280 peaks within each 10-mission block of Tile FLD-2 exceeded 55160 PA (8.0 PSI). The load distribution for Tile FLD-4 more nearly approached the nominal distribution, although a significant increase in peak counts occurred in the 48265 to 55160 Pa (7.0 to 8.0 PSI) stress bin. Only 15 peaks exceeded 55160 Pa (8.0 PSI) for Tile FLD-4.

SIP extension.- SIP extension resulting from the combined load condition was measured by two displacement sensors mounted above but on opposite sides of the tile. SIP extension was measured prior to application of dynamic loading (zero missions) and after each subsequent interval of 50 missions (see test procedure section). The SIP extension data obtained are summarized in Tables IX and X and figures 12 through 17. These data indicate significant SIP extension occurred and generally increased somewhat linearly with respect to the logarithm of the mission exposure. Figures 12 and 15 are plotted in semi-log form to illustrate this point; the remainder are plotted on linear axes. Further, the SIP did not stretch uniformly but varied across the footprint area (see figs. 12 and 15 for example). Maximum measured SIP extension for Tile FLD-2 was 0.556 cm (0.219 inches) on side 1 and 0.345 cm (0.136 inches) on side 2 which gave an average extension of 0.452 cm (0.178 inches) (see fig. 12). For Tile FLD-4 (see fig. 15), the maximum SIP extensions under tension load were 0.48 cm (0.19 inches) on side 1, 0.40 cm (0.16 inches) on side 2 for an average extension of 0.44 cm (0.175 inches). The SIP extensions measured upon removal of the static tension load are shown in figures 12 and 16. Comparisons of the average SIP extension for the loaded and unloaded conditions of Tiles FLD-2 and FLD-4 are given in

figure 17. These data show that the SIP undergoes a steadily increasing permanent set as the number of missions increases. In the case of Tile FLD-2, SIP failure occurred at 710 missions, whereas Tile FLD-4 completed 1500 missions. A photograph of the failure mode of Tile FLD-2 is shown in figure 18. The failure mode in this case was separation at the tile/SIP interface. The photograph also indicates the nonuniform nature of SIP extension at SIP failure.

CONCLUSIONS

Two tests of undensified Space Thuttle thermal protection tiles under combined static and dynamic loads have been conducted. The tiles weighed 144.2 Kg/m^3 (LI 900 tiles) and were mounted on a strain isolator pad which was 0.41 cm (.160 in.) thick. A combined static and dynamic mission stress histogram representative of the W-3 area of the wing of the orbiter vehicle was applied. The stress histogram was provided by the Space Shuttle Project. Pertinent results and comments are summarized below:

1. Tile/SIP response was highly nonlinear at the larger dynamic stress levels and was characterized by sharp tension peaks which could exceed twice the magnitude of the corresponding compression peaks.

2. The nonlinear tile/SIP response properties resulted in overstress of Tile FLD-2 when the standard shaker control system was used. Modification of the controller feedback loop by insertion of a special purpose signal conditioner was effective in reducing the amount of overstress. This situation illustrates a potential problem that must be resolved when designing tests within which tile response is a control parameter.

3. Tile FLD-2, which had an applied static stress of 22409 Pa (3.25 PSI), failed at 710 missions because of separation at the tile/SIP interface. This tile experienced an overstress of approximately 9653 Pa (1.4 PSI) at the high

stress level condition. Tile FLD-4, which had corrected load levels, an applied static stress of 17,237 Pa (2.50 PSI), and an overstress of 2758 Pa (0.40 PSI) completed 1500 missions.

4. The ratio of peak tile acceleration to peak table acceleration was approximately 3.0 for both tiles. The corresponding ratios of RMS tile acceleration to RMS table acceleration was 1.55 for Tile FLD-2 and 1.72 for Tile FLD-4. This difference reflects the nonlinear stress-strain behavior of the SIP.

5. Maximum lateral tile response occurred for Tile FLD-2 and equalled 15 percent of the vertical response. For Tile FLD-4, the maximum lateral response was 3.3 percent of the vertical response. Vertical and lateral response were identical in frequency, although different in waveshape.

6. Significant SIP extension occurred for both tiles because of the static preload and as a result of cycling of the SIP material under dynamic loading. SIP extension gradually increased over mission time, proportionate to the logarithm of the accumulated cyclical loads. The average extension for Tiles FLD-2 and FLD-4 equalled 0.452 cm (0.178 in.) and 0.439 cm (0.173 in.), respectively. Upon removal of the preload, a permanent set remained. This permanent extension of each tile also increased with increased mission time.

APPENDIX

Signal Conditioner Discussion

A block diagram of the acceleration signal conditioner is presented in figure 4. The waveforms shown in this figure represent idealized signals which would typically be present at the points labeled with the same letters in the block diagram, during a time segment equivalent to two tension and one compression half cycle. The accelerometer signal (A) is input to a precision rectifier and a polarity detector. The output of the polarity detector is a digital pulse train of the same frequency as the input, and is a high level when the input is positive and zero level when the input is negative. This pulse train is used for control purposes to be described later.

The rectified signal (B) is an exact duplicate of the input signal, except that the negative portions have been made positive. This wave is modified to a level (C) by the peak hold circuit. This level is exactly as high as the peak of the signal received by the peak hold circuit. The illustration is idealized; a decay rate is built into the peak hold, or else the level could never decrease. In actuality a decay rate slightly greater than the maximum decay rate of the vibration exciter was purposely introduced. This resulted in the actual output level having a slight increase as each tension peak appeared, then a slight decay for approximately 10 ms until the next tension peak.

The level (C) is then sent through two parallel buffers, one of which inverts the signal (D and E). The analog multiplexer selects between these two signals depending upon the instantaneous level of the control signal (F), and applies the proper signal to the output line to obtain a square wave (G)

of the same frequency and phase as the input, but with a magnitude (both positive and negative) as great as the peak positive or negative input occurring in that time segment.

A slight error is present in the output because of the decay built into the peak hold circuit. For purposes of this test the error was calibrated out by varying the gains of the two buffers. This was possible only because of the narrow frequency range required for this test. A more straightforward approach would be to give the peak hold a very long time constant, and reset the peak hold to zero at the beginning of each tension cycle. This approach will be used for any future testing. The vibration controller senses only the fundamental frequency and peak amplitude of the accelerometer signal. Therefore, the fact that the output waveshape of the signal conditioner no longer resembles the input waveshape is of no importance.

REFERENCES

1. Williams, Jerry G.: Structural Tests on a Tile/Strain Isolation Pad Thermal Protection System. NASA TM 80226, March 1980.
2. Sawyer, J. W.; and Rummler, D. R.: Room Temperature Mechanical Properties of Shuttle Thermal Protection System Materials. NASA TM 81786, April 1980.
3. Williams, Jerry G.: Structural Tests on Space Shuttle Thermal Protection System Constructed with Nondensified and Densified LI 900 and LI 2200 Tile. NASA TM 81903, January 1981.
4. Miserentino, R.; Pinson, L. D.; and Leadbetter, S. A.: Some Space Shuttle Tile/Strain-Isolator-Pad Sinusoidal Tests. NASA TM 81853, July 1980.
5. Sawyer, J. W.; and Cooper, P. A.: Fatigue Properties of Shuttle Thermal Protection System. NASA TM 81899, November 1980.

TABLE I.- PEAK ACCELERATION LEVELS IN COMPRESSION AND TENSION FOR TEST FLD-2

(a) COMPRESSION PEAKS, G

NUMBER OF MISSIONS	VERT ACCEL 1	VERT ACCEL 2	VERT ACCEL 3	VERT ACCEL 4	LAT ACCEL 1	LAT ACCEL 2	TABLE ACCEL	AVG VERT G
100	15.64	18.09	18.06	15.81	2.28	1.06	13.19	16.90
150	16.06	18.38	18.52	16.50	2.30	1.22	13.20	17.36
200	16.10	18.30	18.47	16.71	2.36	1.14	13.26	17.39
350	16.06	18.04	18.36	15.14	2.32	1.37	13.98	16.90
450	15.95	17.67	17.68	15.03	2.28	1.51	13.37	16.58
550	15.72	16.98	17.46	15.65	2.13	1.35	13.52	16.45
650	16.08	16.91	17.11	15.76	2.20	1.31	13.38	16.46
AVG=	15.94	17.76	17.95	15.80	2.26	1.28	13.41	16.86

(b) TENSION PEAKS, G

NUMBER OF MISSIONS	VERT ACCEL 1	VERT ACCEL 2	VERT ACCEL 3	VERT ACCEL 4	LAT ACCEL 1	LAT ACCEL 2	TABLE ACCEL	AVG VERT G
100	34.57	36.67	34.74	34.62	5.54	2.22	11.67	35.15
150	34.34	36.29	34.65	34.54	5.13	1.93	12.04	34.96
200	34.26	36.52	34.92	34.60	5.28	2.10	12.38	35.08
350	35.01	36.63	34.76	34.17	5.13	1.71	12.18	35.14
450	34.59	36.36	34.81	33.87	5.04	1.59	11.62	34.91
550	35.51	36.82	35.55	34.41	5.47	1.61	12.18	35.57
650	35.34	36.82	35.45	34.51	5.40	1.46	11.53	35.53
AVG=	34.80	36.59	34.98	34.38	5.28	1.80	11.94	35.19

TABLE II.- PEAK ACCELERATION LEVELS IN COMPRESSION AND TENSION FOR TEST FLD-4

(a) COMPRESSION PEAKS, G

NUMBER OF MISSIONS	VERT ACCEL 1	VERT ACCEL 2	VERT ACCEL 3	VERT ACCEL 4	LAT ACCEL 1	LAT ACCEL 2	TABLE ACCEL	AVG VERT G
100	10.30	11.01	10.76	10.44	---	---	11.23	10.62
300	11.28	11.54	12.04	11.42	.265	.906	11.83	11.57
500	11.59	12.18	12.48	12.08	.306	.906	10.81	12.08
700	10.92	11.68	11.53	11.06	.195	.719	11.53	11.30
900	10.79	11.40	11.37	10.95	.438	.739	11.16	11.13
1100	11.00	11.76	11.85	11.52	.417	.788	11.87	11.53
1300	11.02	11.84	12.12	11.66	.326	.857	11.72	11.66
1500	10.81	11.44	11.51	11.12	.205	.847	11.56	11.22
AVG=	10.96	11.61	11.71	11.28	.307	.822	11.46	11.39

(b) TENSION PEAKS, G

NUMBER OF MISSIONS	VERT ACCEL 1	VERT ACCEL 2	VERT ACCEL 3	VERT ACCEL 4	LAT ACCEL 1	LAT ACCEL 2	TABLE ACCEL	AVT VERT G
100	32.66	31.79	32.54	33.23	---	---	10.75	32.56
300	33.28	33.77	36.27	34.64	.393	1.248	11.00	34.49
500	30.07	30.33	33.16	31.23	.342	.954	10.23	31.20
700	33.00	32.94	34.19	33.34	.402	1.218	10.78	33.37
900	31.25	30.33	32.40	31.56	.463	1.081	10.56	31.38
1100	33.50	31.85	34.74	33.59	.544	1.042	11.58	33.42
1300	33.79	34.32	37.23	35.33	.453	1.051	11.29	35.17
1500	32.93	31.32	33.16	32.63	.443	1.012	10.97	32.51
AVG=	32.56	32.08	34.21	33.19	.434	1.086	10.90	33.01

TABLE III.- MAXIMUM RMS ACCELERATION LEVELS FOR TESTS FLD-2 AND FLD-4 (IN G UNITS)

(a) FLD-2

NUMBER OF MISSIONS	VERT ACCEL 1	VERT ACCEL 2	VERT ACCEL 3	VERT ACCEL 4	LAT ACCEL 1	LAT ACCEL 2	TABLE ACCEL	AVG VERT G
100	10.54	11.03	11.12	10.55	1.51	.653	7.04	10.81
150	11.54	12.14	12.26	11.72	1.61	.686	7.74	11.92
200	11.14	11.62	11.77	11.30	1.54	.656	7.52	11.46
350	10.36	10.80	10.94	9.79	1.42	.587	6.83	10.47
450	11.04	11.48	11.64	10.42	1.51	.669	7.26	11.14
550	10.82	11.19	11.34	10.70	1.48	.655	7.01	11.01
650	10.79	11.10	11.19	10.72	1.46	.632	6.88	10.95
AVG=	10.89	11.34	11.46	10.74	1.50	.648	7.18	11.10

(b) FLD-4

NUMBER OF MISSIONS	VERT ACCEL 1	VERT ACCEL 2	VERT ACCEL 3	VERT ACCEL 4	LAT ACCEL 1	LAT ACCEL 2	TABLE ACCEL	AVG VERT G
100	12.59	12.73	12.81	12.75	.113	.619	7.46	12.72
300	13.04	13.32	13.70	13.39	.101	.548	7.73	13.36
500	12.48	12.84	13.26	12.96	.112	.504	7.40	12.88
700	12.81	12.73	12.59	12.86	.118	.488	7.51	12.75
900	13.04	13.20	13.59	13.39	.135	.504	7.73	13.30
1100	12.81	12.73	13.26	13.18	.146	.482	7.46	13.00
1300	12.81	13.08	13.59	13.28	.140	.488	7.57	13.19
1500	12.70	12.37	12.37	12.75	.146	.460	7.40	12.55
AVG=	12.78	12.88	13.15	13.07	.126	.512	7.53	12.97

TABLE IV.- RATIO OF PEAK AND RMS ACCELERATION RESPONSE TO PEAK AND RMS TABLE INPUT FOR THE HIGH STRESS LEVEL CONDITION IN TESTS FLD-2 AND FLD-4.

(a) FLD-2; σ_{static} = 22,408 Pa (3.25 PSI)

ACCELEROMETER	(PEAK) OUT/(PEAK) IN	(RMS) OUT/(RMS) IN
VERT 1	2.92	1.52
VERT 2	3.07	1.58
VERT 3	2.94	1.60
VERT 4	2.88	1.50
AVERAGE	2.95	1.55

(b) FLD-4; σ_{static} = 17,237 Pa (2.50 PSI)

ACCELEROMETER	(PEAK) OUT/(PEAK) IN	(RMS) OUT/(RMS) IN
VERT 1	2.98	1.70
VERT 2	2.94	1.70
VERT 3	3.14	1.75
VERT 4	3.04	1.74
AVERAGE	3.02	1.72

TABLE V.- RATIO OF AVERAGE PEAK ACCELERATION TO AVERAGE RMS ACCELERATION FOR TESTS FLD-2 AND FLD-4. (AVERAGE TAKEN OVER MISSION TIME, SEE TABLES I, II, III); ACCELERATION IN G's)

	PEAK ACCELERATION		RMS ACCELERATION		(PEAK)/(RMS)	
ACCELEROMETER	FLD-2	FLD-4	FLD-2	FLD-4	FLD-2	FLD-4
VERT 1	34.80	32.56	10.89	12.78	3.20	2.55
VERT 2	36.59	32.08	11.34	12.88	3.23	2.49
VERT 3	34.98	34.21	11.46	13.15	3.05	2.60
VERT 4	34.38	33.19	10.74	13.07	3.20	2.54

TABLE VI.- RATIO OF AVERAGE PEAK LATERAL RESPONSE TO AVERAGE PEAK VERTICAL RESPONSE FOR TESTS FLD-2 AND FLD-4. (LATERAL RESPONSE AVERAGED OVER MISSION TIME, VERTICAL RESPONSE AVERAGED OVER MISSION TIME AND ACCELEROMETER LOCATION.)

ACCELEROMETER	FLD-2 σ_{static} = 22,408 Pa (3.25 PSI)	FLD-4 σ_{static} = 17,237 Pa (2.50 PSI)
LAT 1	0.150	0.013
LAT 2	0.051	0.033

TABLE VII.- PEAK SIP STRESS LEVELS IN COMPRESSION AND TENSION FOR TESTS FLD-2 AND FLD-4. STRESSES IN PSI

(a) FLD-2

ACCELEROMETER	COMPRESSION, PSI	TENSION, PSI
VERT 1	.473	9.31
VERT 2	.156	9.62
VERT 3	.123	9.34
VERT 4	.497	9.24
AVG STRESS=	.312	9.38

$R_{AVG} = \sigma_{TENS}/\sigma_{COMP} = 0.033$

(b) FLD-4

ACCELEROMETER	COMPRESSION, PSI	TENSION, PSI
VERT 1	.541	8.32
VERT 2	.424	8.23
VERT 3	.407	8.61
VERT 4	.484	8.43
AVG STRESS=	.464	8.40

$R_{AVG} = \sigma_{TENS}/\sigma_{COMP} = 0.055$

TABLE VIII.- DISTRIBUTION OF PEAK STRESS FOR TESTS FLD-2 AND FLD-4. STRESSES IN PSI

(a) FLD-2

STRESS RANGE psi	MISSIONS 41-50	MISSIONS 691-700	DESIRED
2.0 - 3.0	---	---	---
3.0 - 4.0	262	312	---
4.0 - 5.0	2433	2299	2740
5.0 - 6.0	8515	8902	12540
6.0 - 7.0	7106	6714	6180
7.0 - 8.0	3653	3775	360
8.0 - 9.0	262	256	---
9.0 - 10.0	21	23	---
TOTAL	22252	22281	21820

(b) FLD-4

STRESS RANGE psi	MISSIONS 41-50	MISSIONS 1491-1500	DESIRED
2.0 - 3.0	44	---	---
3.0 - 4.0	113	175	---
4.0 - 5.0	3230	2390	2740
5.0 - 6.0	12018	12809	12540
6.0 - 7.0	6353	5833	6180
7.0 - 8.0	1013	1097	360
8.0 - 9.0	15	15	---
9.0 - 10.0	---	---	---
TOTAL	22786	22319	21820

TABLE IX.- ABSOLUTE AND RELATIVE SIP EXTENSION FOR TEST FLD-2. (ALL DISPLACEMENTS IN CM)

	ABSOLUTE						RELATIVE		
NUMBER OF MISSIONS	LOADED DISPL 1	LOADED DISPL 2	AVERAGE LOADED DISPL	UNLOADED DISPL 1	UNLOADED DISPL 2	AVERAGE UNLOADED DISPL	Δ DISPL 1	Δ DISPL 2	AVERAGE Δ DISPL
0	.163	.119	.142	0	0	0	0	0	0
50	.300	.193	.246	.213	.099	.157	.137	.074	.107
100	.330	.208	.269	.246	.122	.183	.168	.089	.127
150	.353	.224	.290	.279	.142	.211	.191	.104	.147
200	.373	.239	.305	.302	.152	.229	.211	.119	.165
250	.399	.259	.330	.330	.183	.257	.236	.140	.188
300	.396	.251	.325	.315	.163	.239	.234	.132	.183
350	.419	.267	.343	.323	.165	.244	.254	.147	.201
400	.434	.282	.358	.351	.193	.272	.272	.163	.218
450	.450	.295	.371	.373	.208	.290	.287	.175	.231
500	.460	.300	.381	.401	.229	.315	.297	.180	.239
550	.472	.305	.389	.389	.216	.302	.310	.185	.249
600	.490	.320	.406	.411	.229	.320	.328	.201	.264
650	.513	.330	.422	.424	.244	.335	.351	.211	.279
700	.556	.345	.452	.462	.254	.358	.394	.226	.284

TABLE X.- ABSOLUTE AND RELATIVE SIP EXTENSION FOR TEST FLD-4. (ALL DISPLACEMENTS IN CM)

	ABSOLUTE						RELATIVE		
NUMBER OF MISSIONS	LOADED DISPL 1	LOADED DISPL 2	AVERAGE LOADED DISPL	UNLOADED DISPL 1	UNLOADED DISPL 2	AVERAGE UNLOADED DISPL	Δ DISPL 1	Δ DISPL 2	AVERAGE Δ DISPL
0	.165	.135	.150	0	0	0	0	0	0
50	.277	.231	.254	.168	.155	.163	.112	.099	.104
100	.318	.267	.292	.206	.175	.191	.152	.132	.142
150	.340	.284	.312	.239	.198	.218	.175	.150	.163
200	.356	.297	.325	.244	.203	.224	.191	.163	.178
250	.368	.305	.335	.257	.218	.239	.203	.170	.188
300	.386	.320	.353	.282	.239	.259	.221	.185	.203
350	.391	.323	.356	.287	.241	.264	.226	.188	.208
400	.406	.338	.371	.335	.279	.307	.241	.203	.224
450	.411	.343	.376	.310	.264	.287	.246	.208	.229
500	.417	.348	.381	.315	.269	.292	.251	.213	.234
550	.406	.335	.371	.315	.259	.287	.241	.201	.221
600	.424	.353	.389	.305	.257	.279	.259	.218	.239
650	.427	.353	.391	.310	.262	.284	.262	.218	.241
700	.429	.356	.394	.315	.262	.290	.264	.221	.244
750	.422	.348	.386	.305	.251	.279	.257	.213	.234

TABLE X.- CONCLUDED

NUMBER OF MISSIONS	ABSOLUTE						RELATIVE		
	LOADED		AVERAGE LOADED	UNLOADED		AVERAGE UNLOADED			
	DISPL 1	DISPL 2	DISPL	DISPL 1	DISPL 2	DISPL	Δ DISPL 1	Δ DISPL 2	AVERAGE Δ DISPL
800	.432	.358	.396	.323	.267	.295	.267	.224	.244
850	.439	.363	.401	.333	.274	.305	.274	.229	.251
900	.442	.361	.401	.330	.274	.302	.277	.226	.251
950	.450	.371	.411	.343	.279	.310	.284	.236	.259
1000	.452	.363	.406	.338	.277	.307	.287	.229	.259
1050	.452	.368	.411	.353	.290	.320	.287	.234	.262
1100	.452	.371	.411	.356	.295	.325	.287	.236	.262
1150	.455	.373	.414	.338	.284	.310	.290	.239	.264
1200	.460	.376	.417	.401	.325	.363	.295	.241	.269
1250	.465	.384	.424	.414	.335	.376	.300	.249	.274
1300	.470	.384	.427	.414	.335	.376	.305	.249	.277
1350	.472	.386	.429	.419	.340	.381	.307	.251	.279
1400	.470	.373	.422	.417	.335	.376	.305	.239	.272
1450	.483	.391	.437	.429	.343	.386	.318	.257	.287
1500	.485	.394	.439	.432	.348	.391	.320	.259	.290

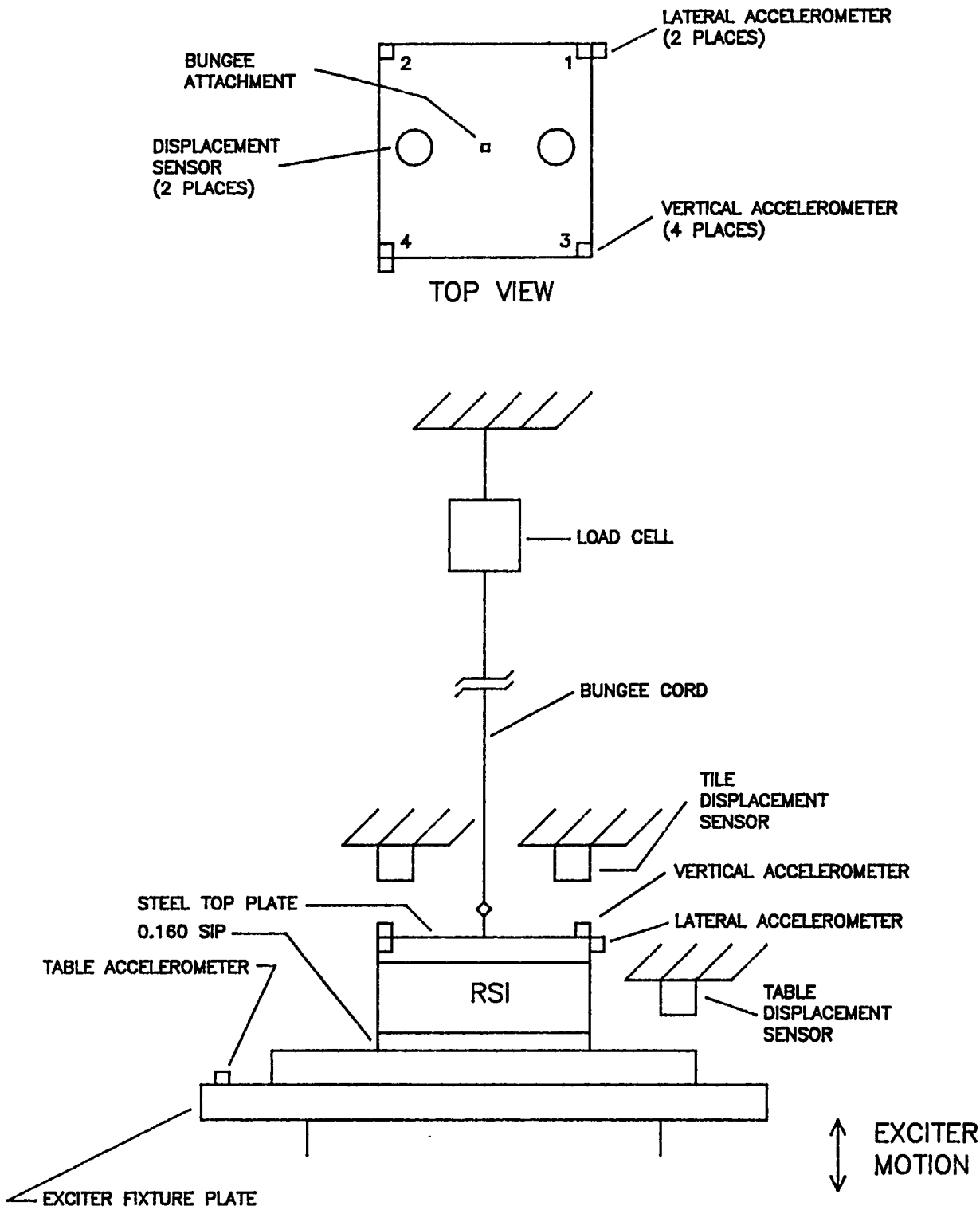

FIGURE 1.- TEST SETUP.

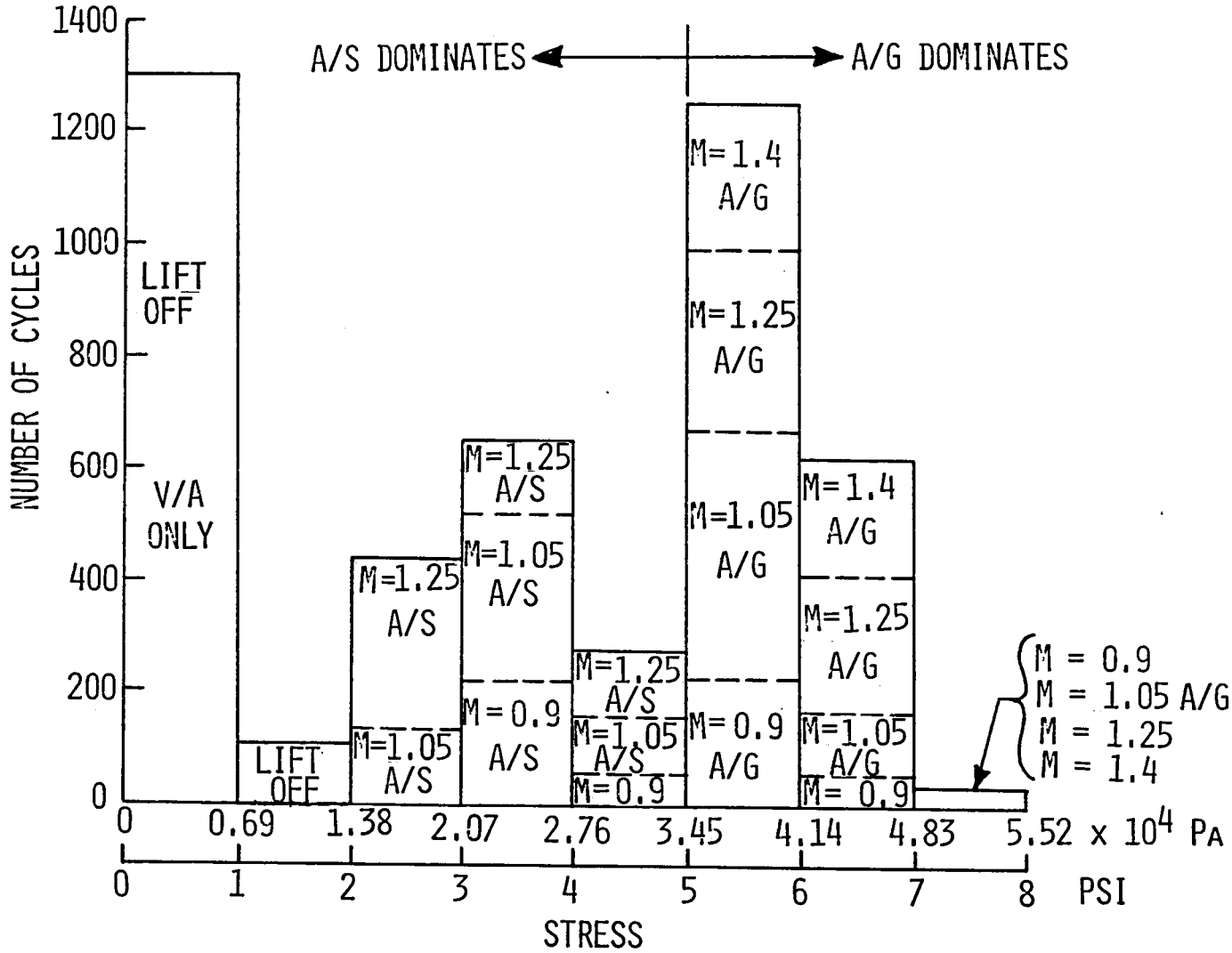

FIGURE 2.- STRESS HISTOGRAM SUPPLIED BY SHUTTLE PROJECT (ONLY STRESS BINS BETWEEN 20.7 AND 55.2 KPA WERE USED IN TESTS).

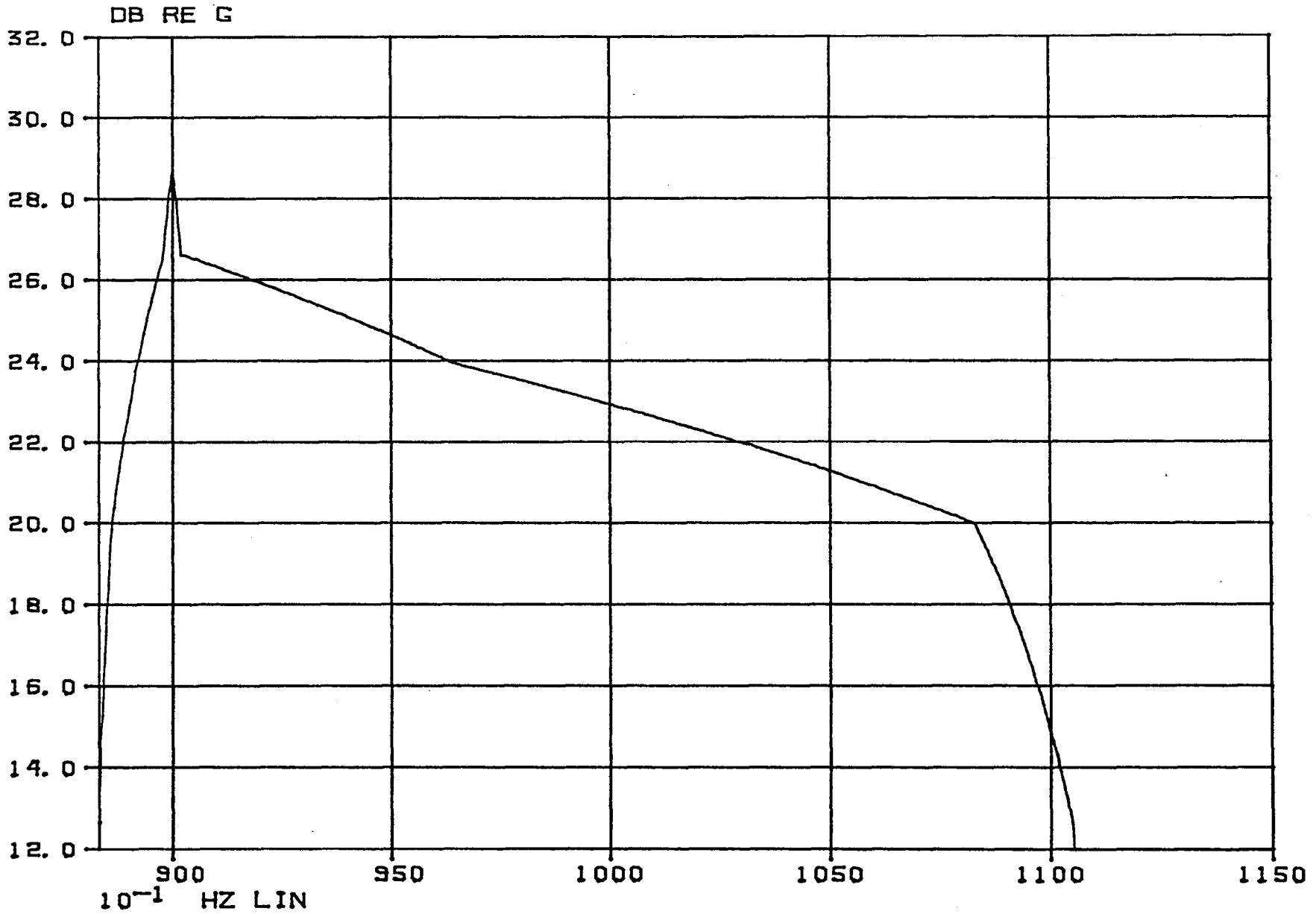

FIGURE 3.- REFERENCE SPECTRUM

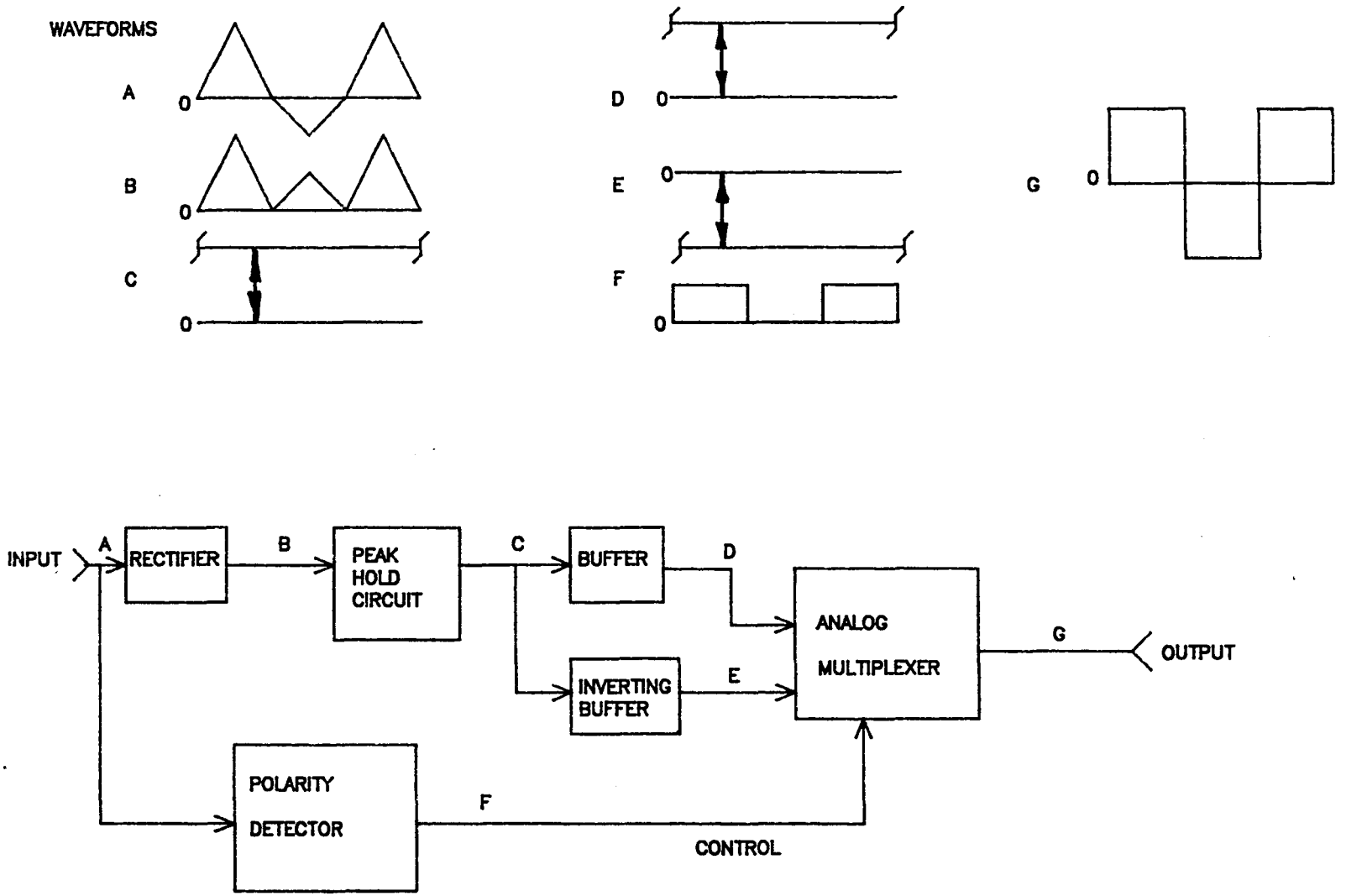

FIGURE 4.- SIGNAL CONDITIONER

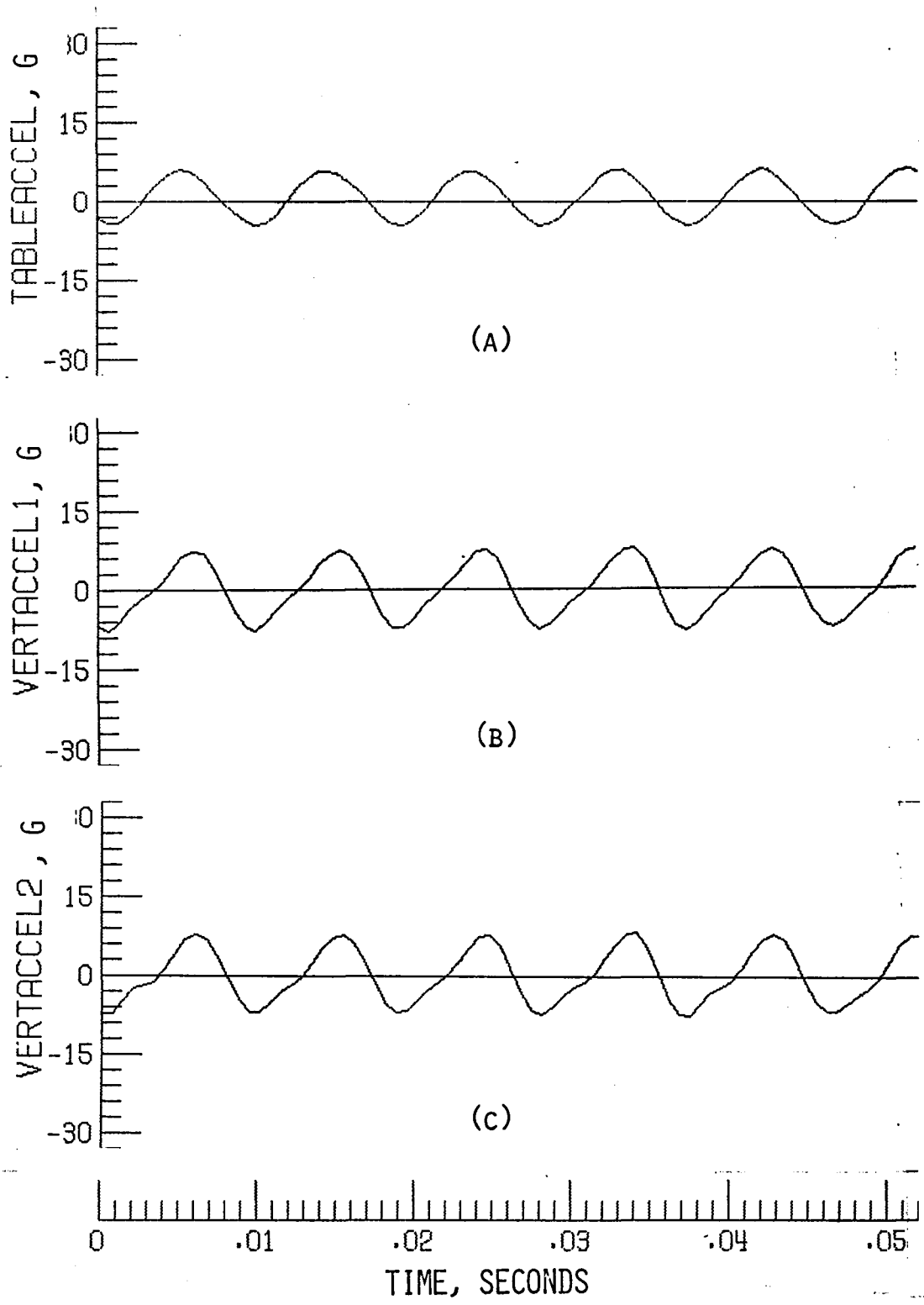

FIGURE 5.- RESPONSE TIME HISTORIES FOR TILE FLD-2 AT A LOW DYNAMIC STRESS LEVEL.

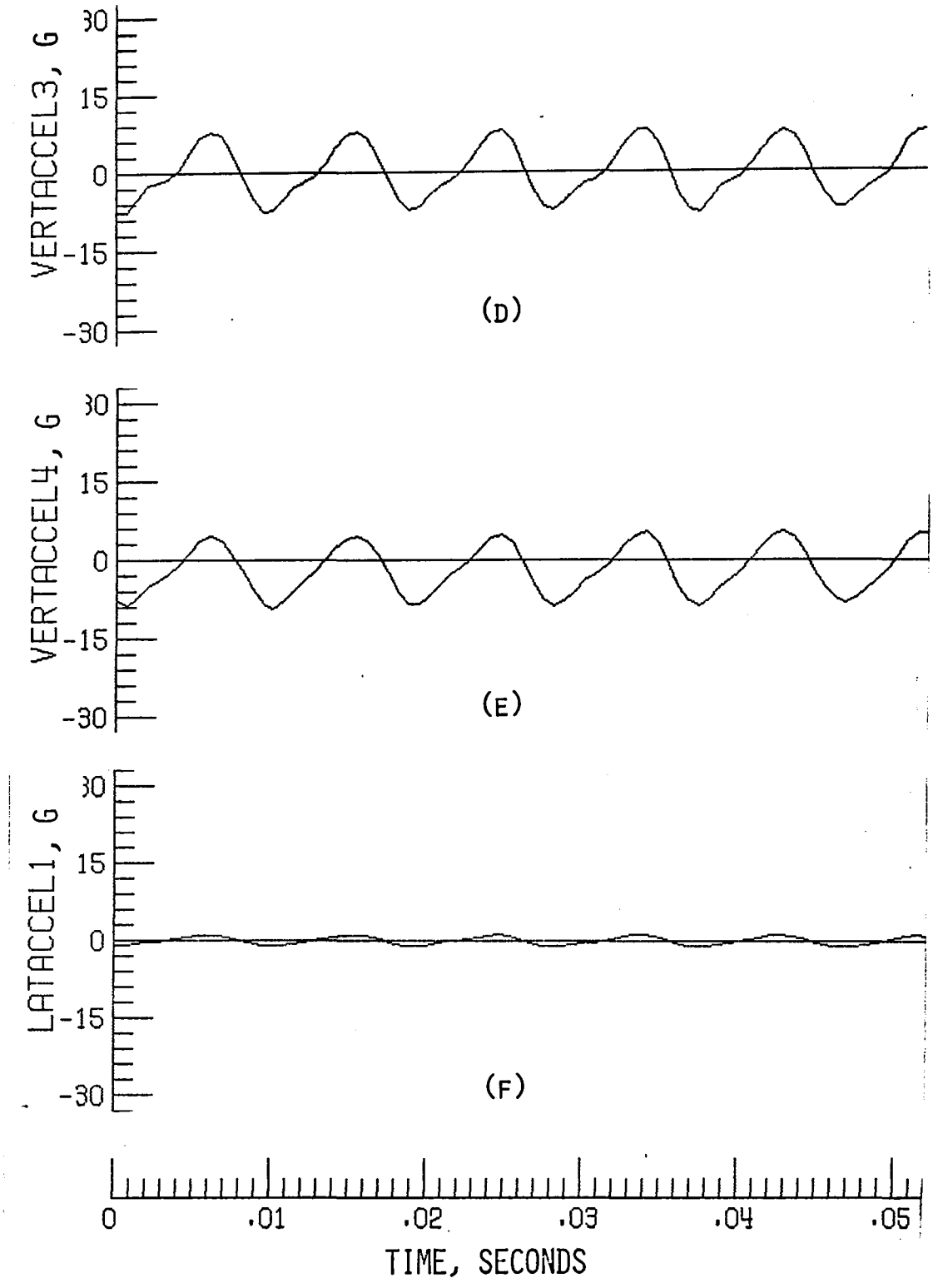

FIGURE 5.- CONCLUDED.

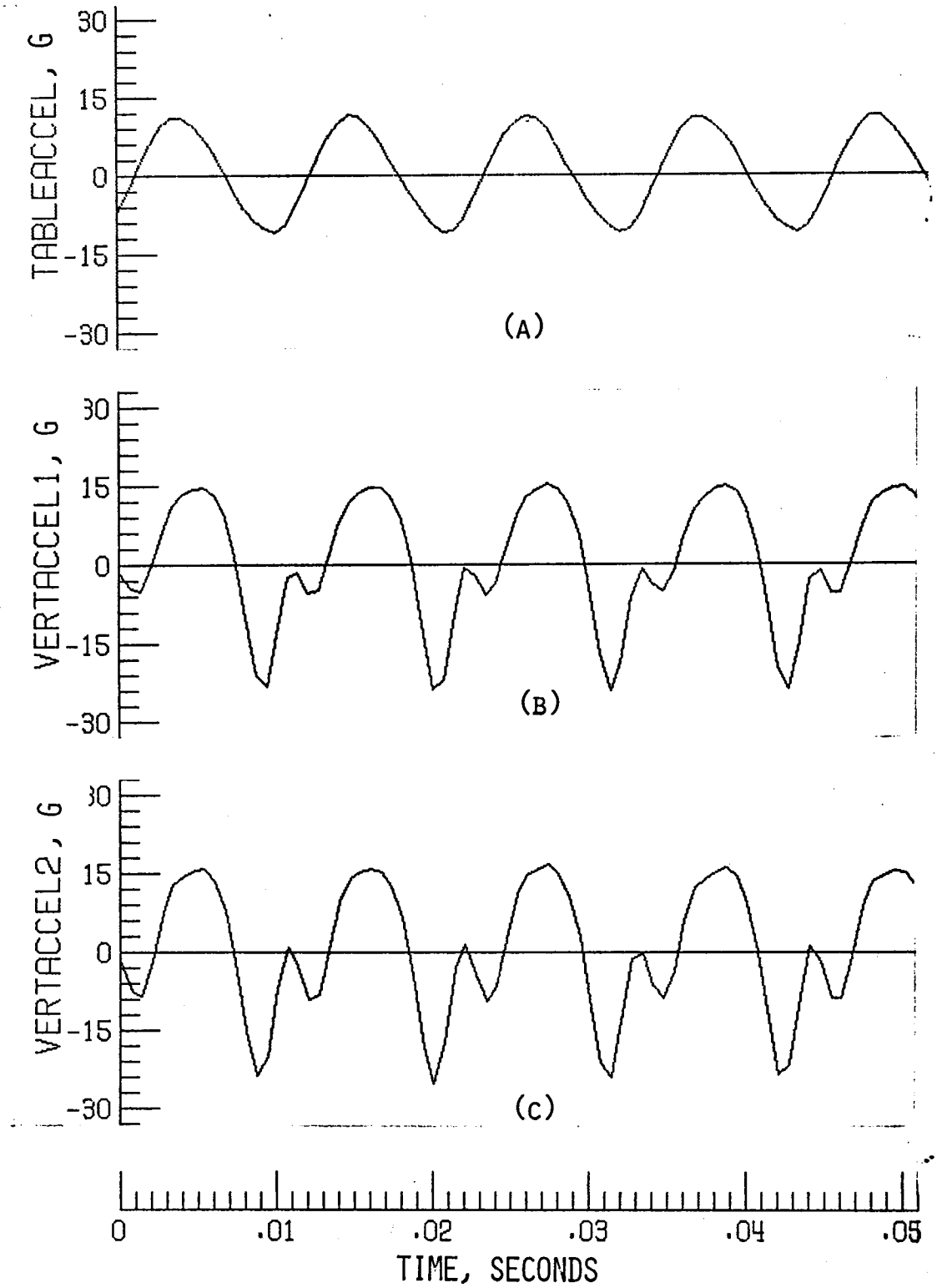

FIGURE 6.- RESPONSE TIME HISTORIES FOR TILE FLD-2 AT A HIGH DYNAMIC STRESS LEVEL.

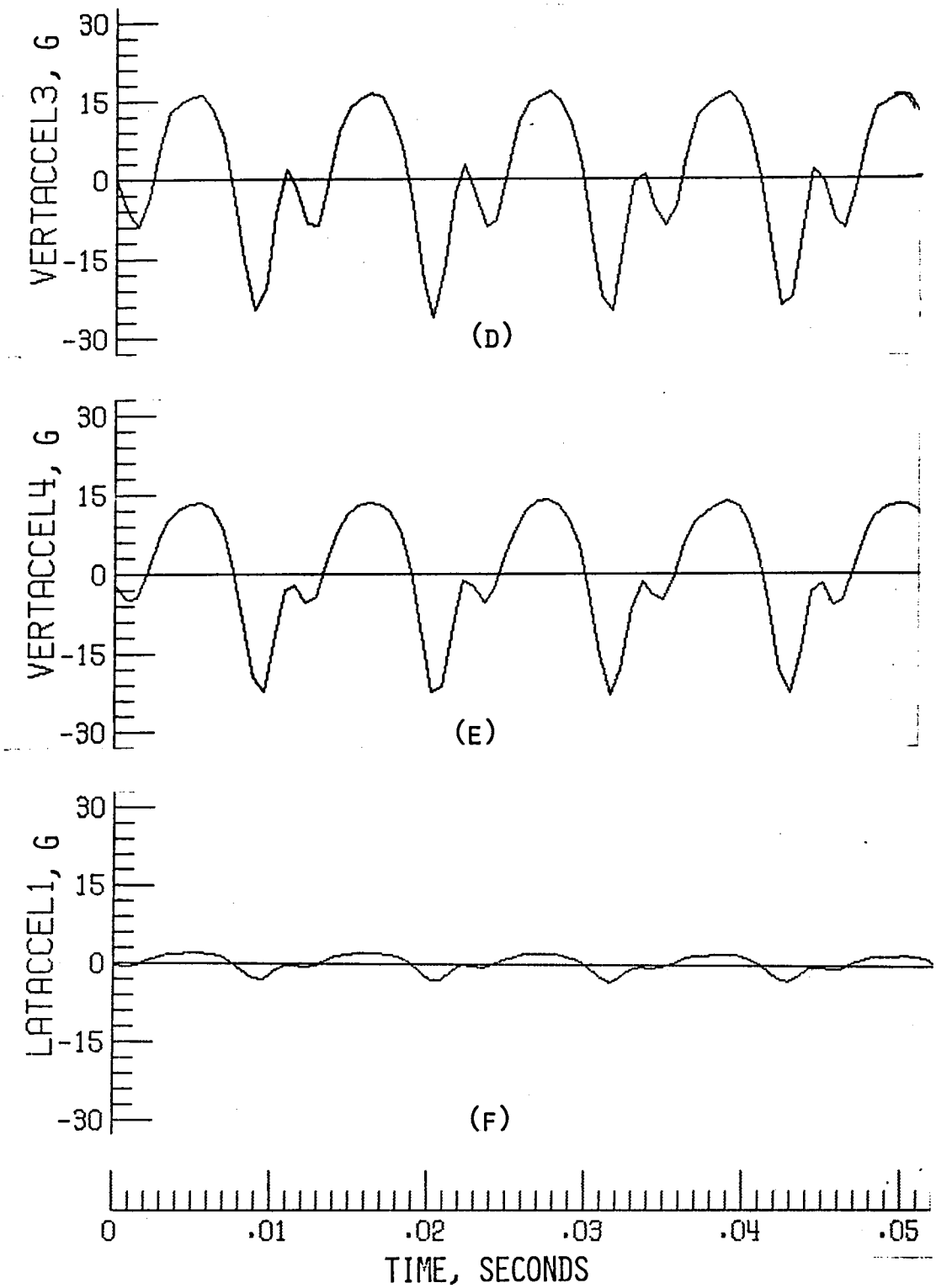

FIGURE 6.- CONCLUDED.

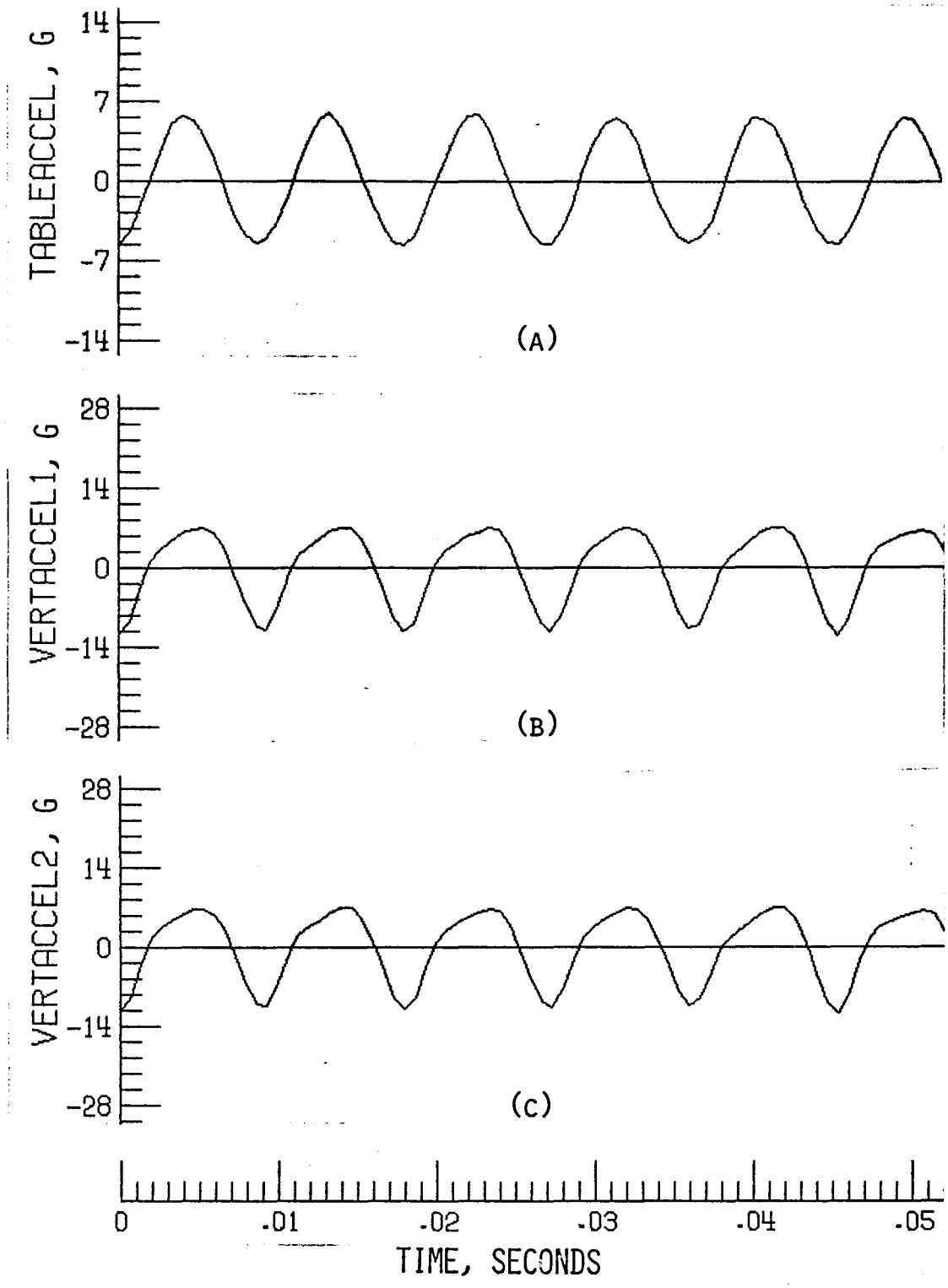

FIGURE 7.- RESPONSE TIME HISTORIES FOR TILE FLD-4 AT A LOW DYNAMIC STRESS LEVEL.

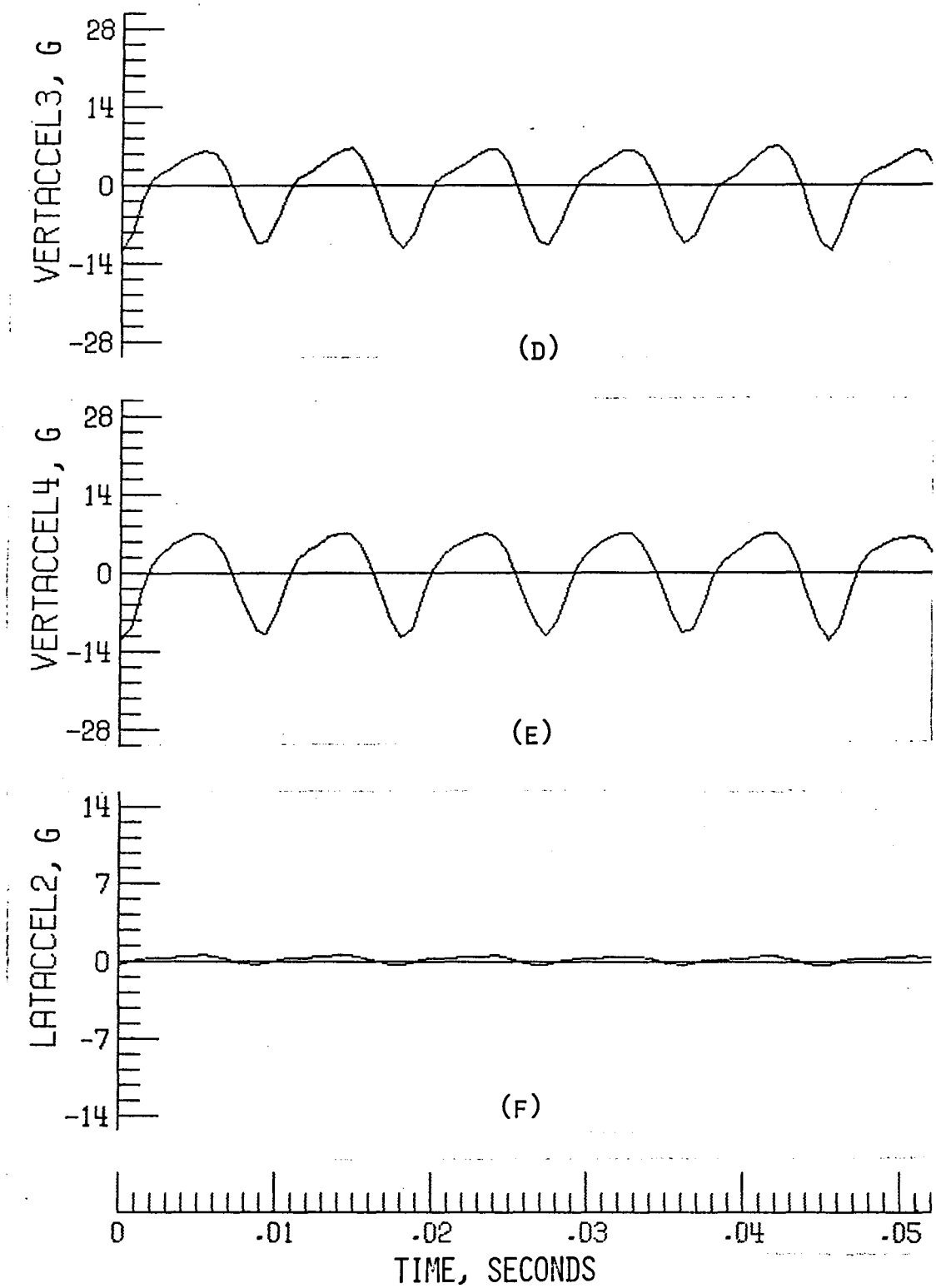

FIGURE 7.- CONCLUDED.

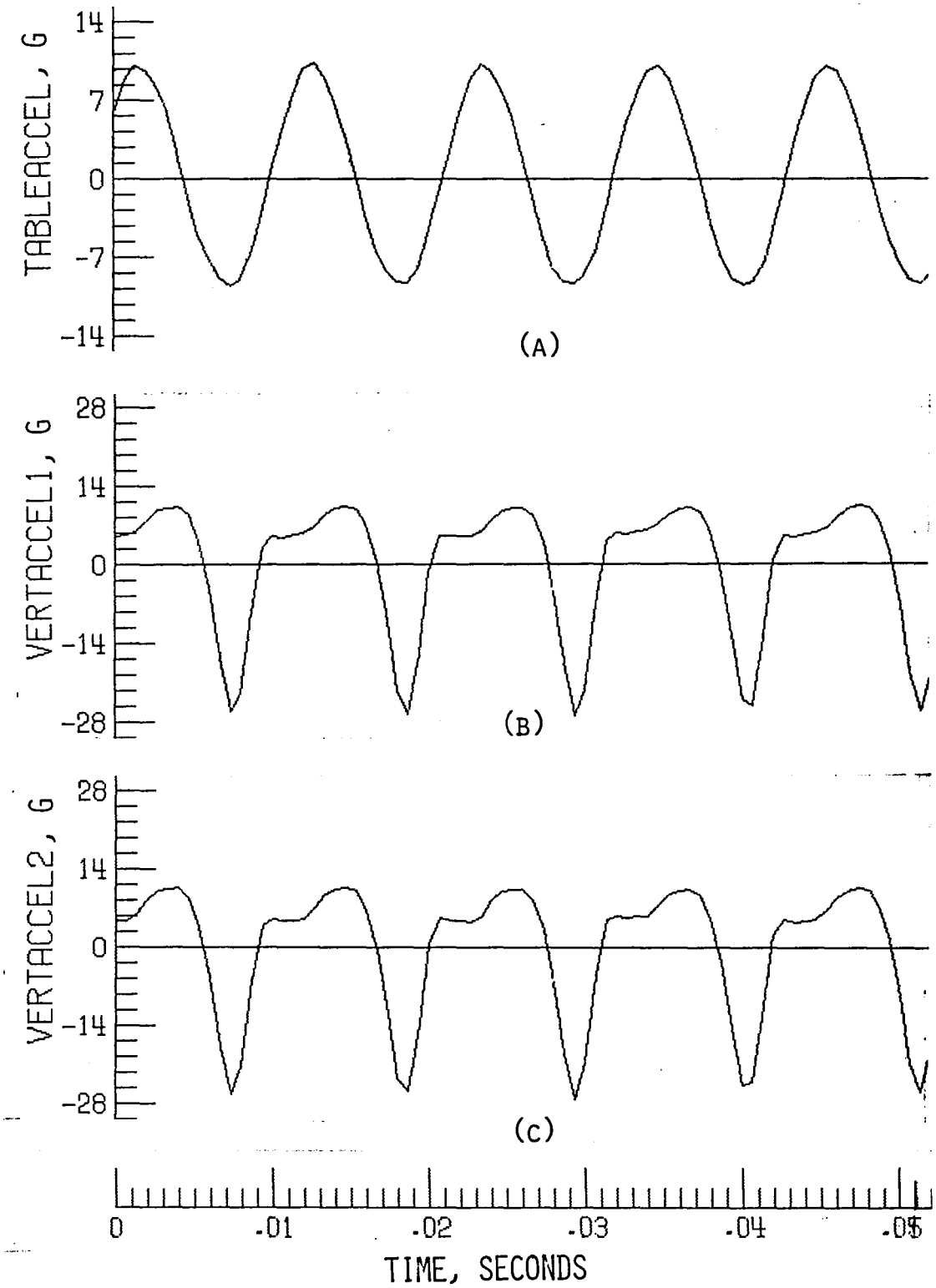

FIGURE 8.- RESPONSE TIME HISTORIES FOR TILE FLD-4 AT A HIGH DYNAMIC STRESS LEVEL.

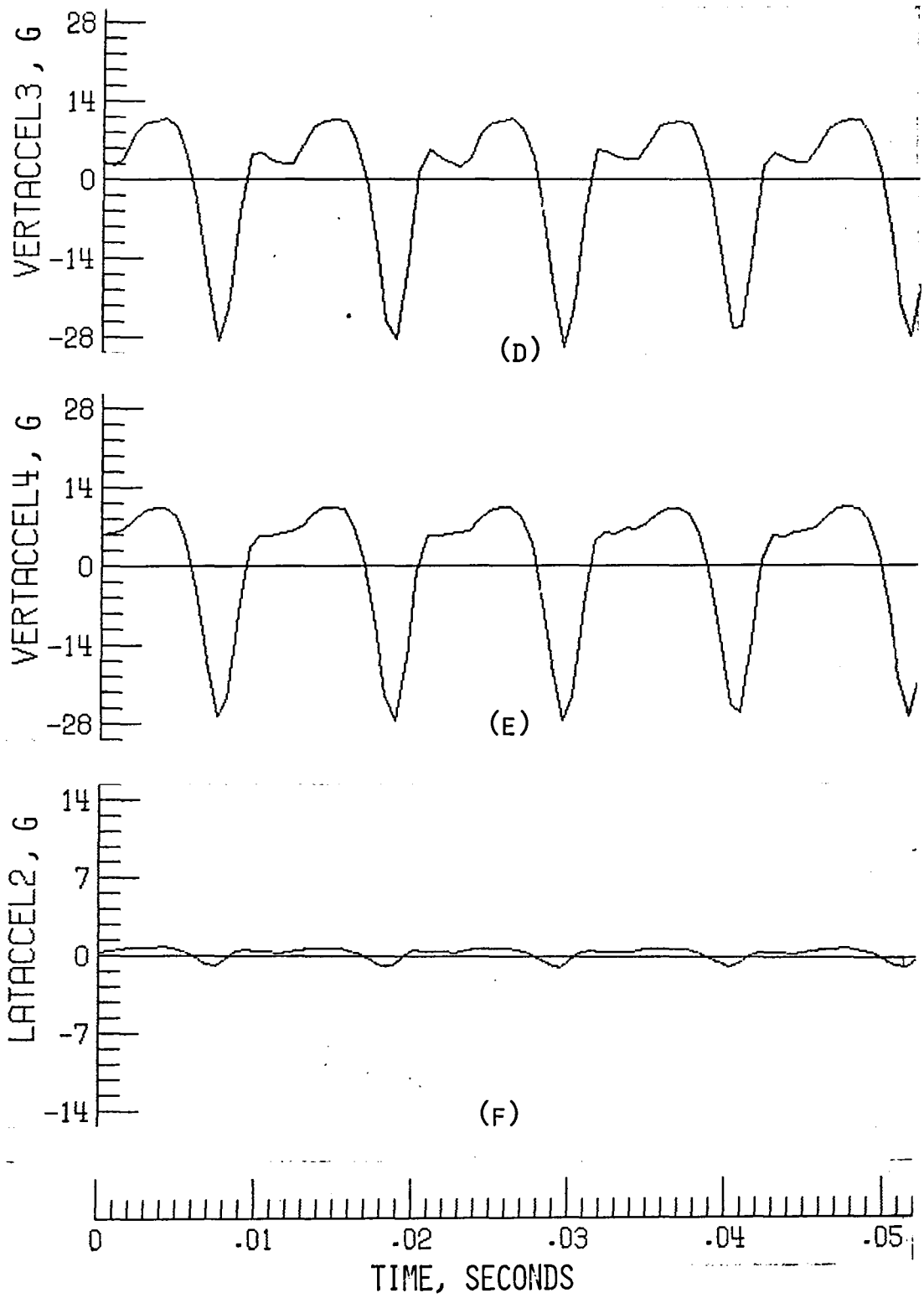

FIGURE 8.- CONCLUDED

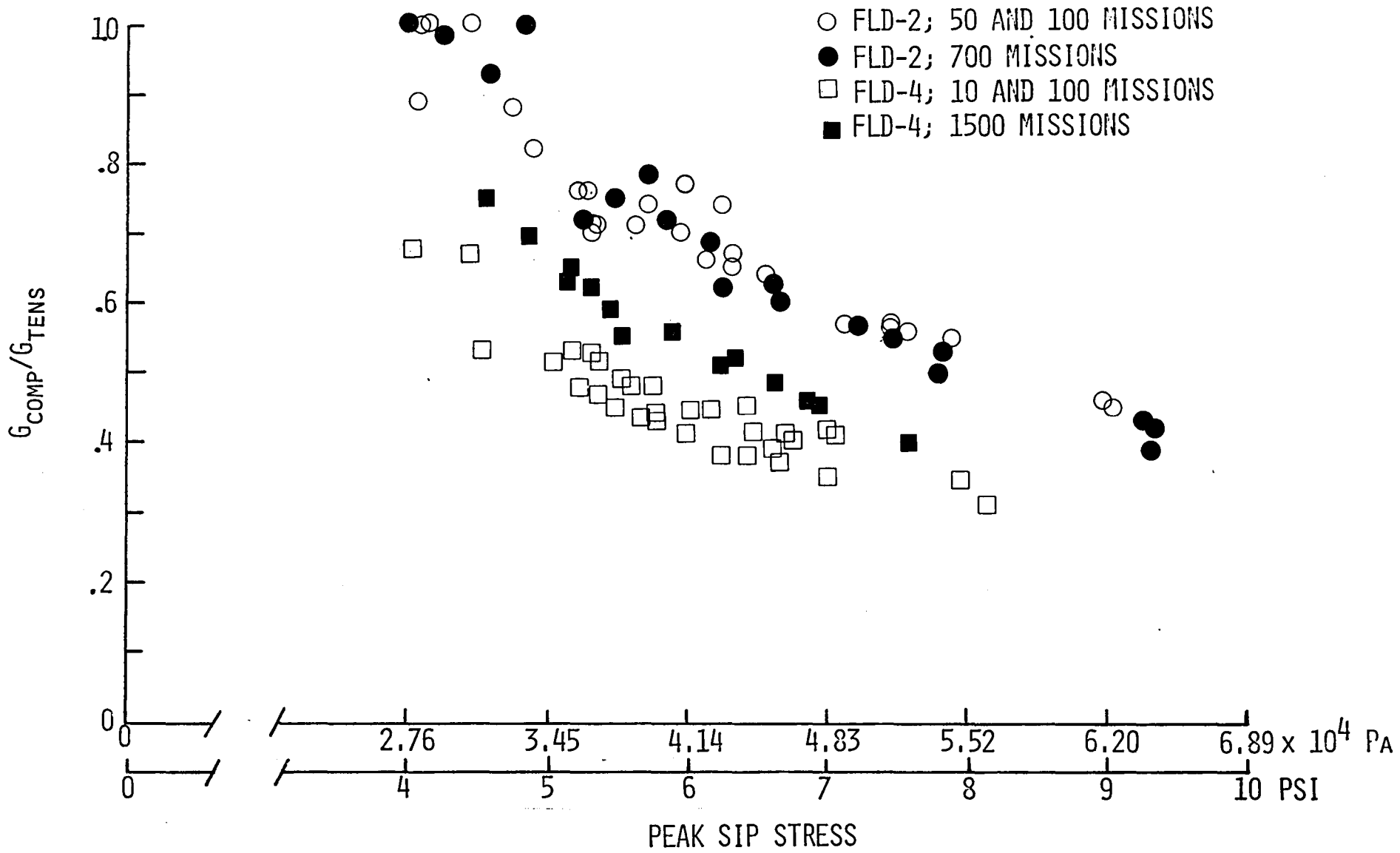

FIGURE 9.- RATIO OF COMPRESSIVE ACCELERATION TO TENSION ACCELERATION FOR TILES FLD-2 AND FLD-4.

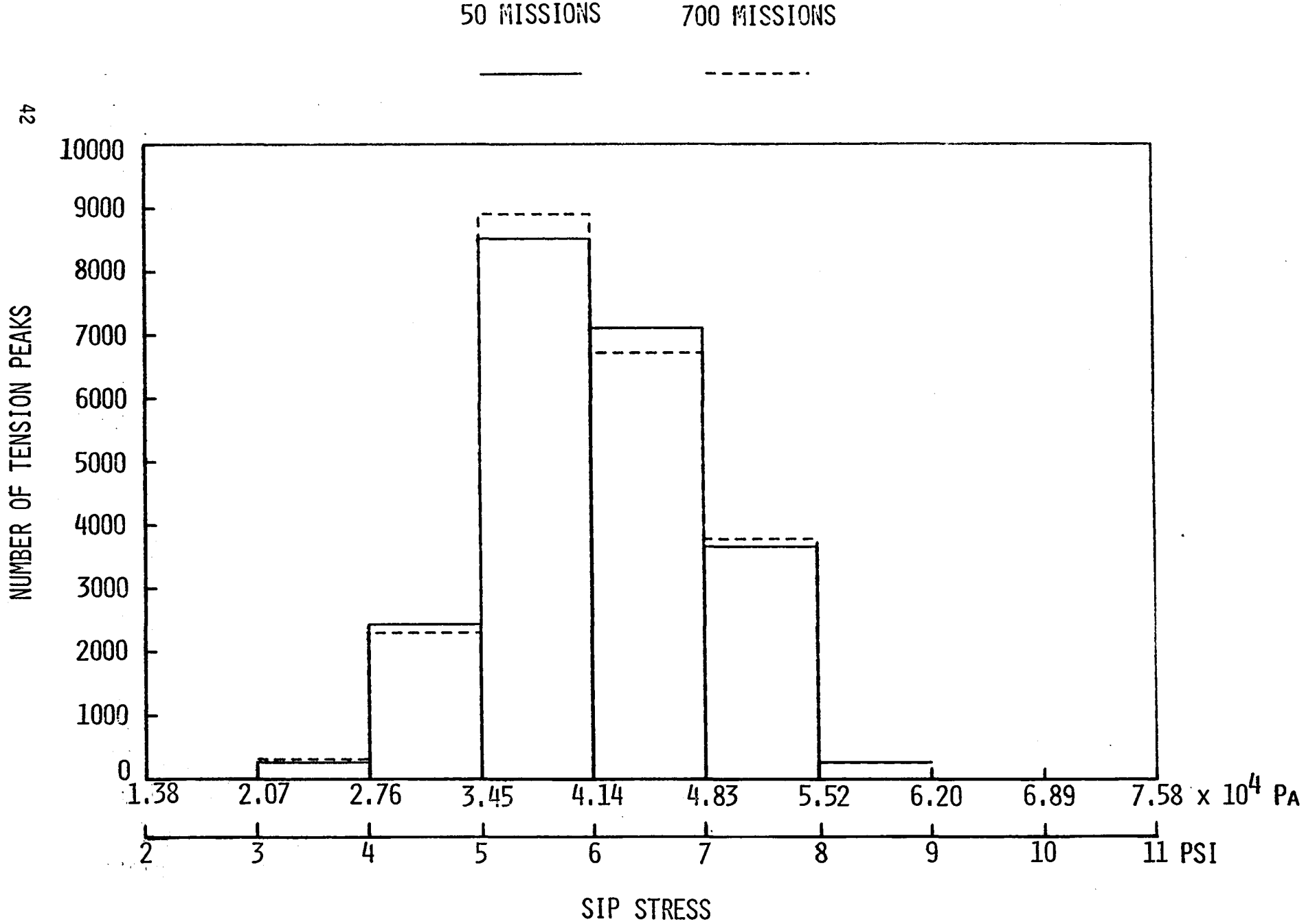

FIGURE 10.- PEAK STRESS HISTOGRAM FOR TILE FLD-2.

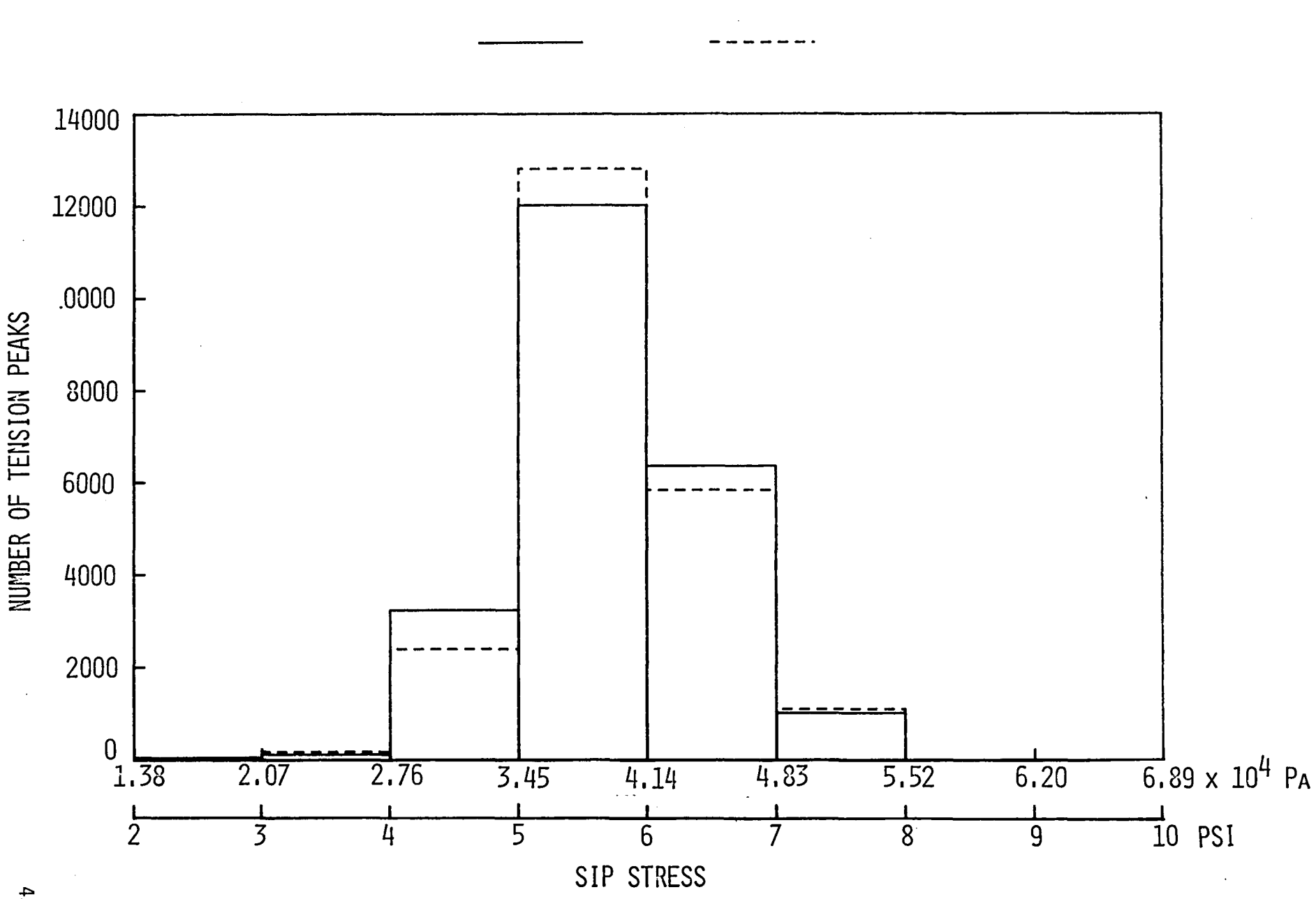

FIGURE 11.- PEAK STRESS HISTOGRAM FOR TILE FLD-4.

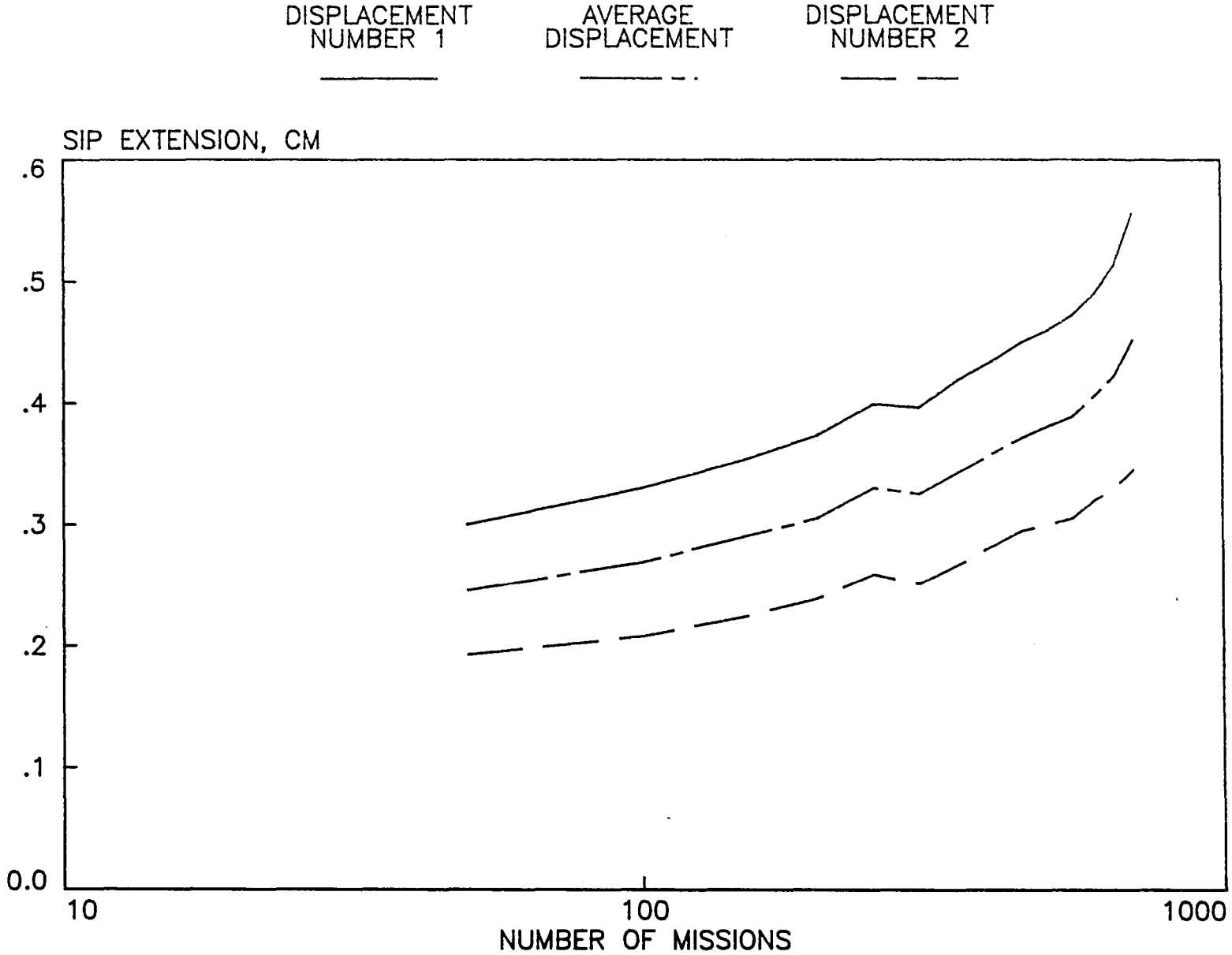

FIGURE 12.- ABSOLUTE SIP EXTENSION FOR TILE FLD-2 AD A FUNCTION OF THE NUMBER OF SIMULATED MISSIONS (STATIC STRESS = 22.4 KPA).

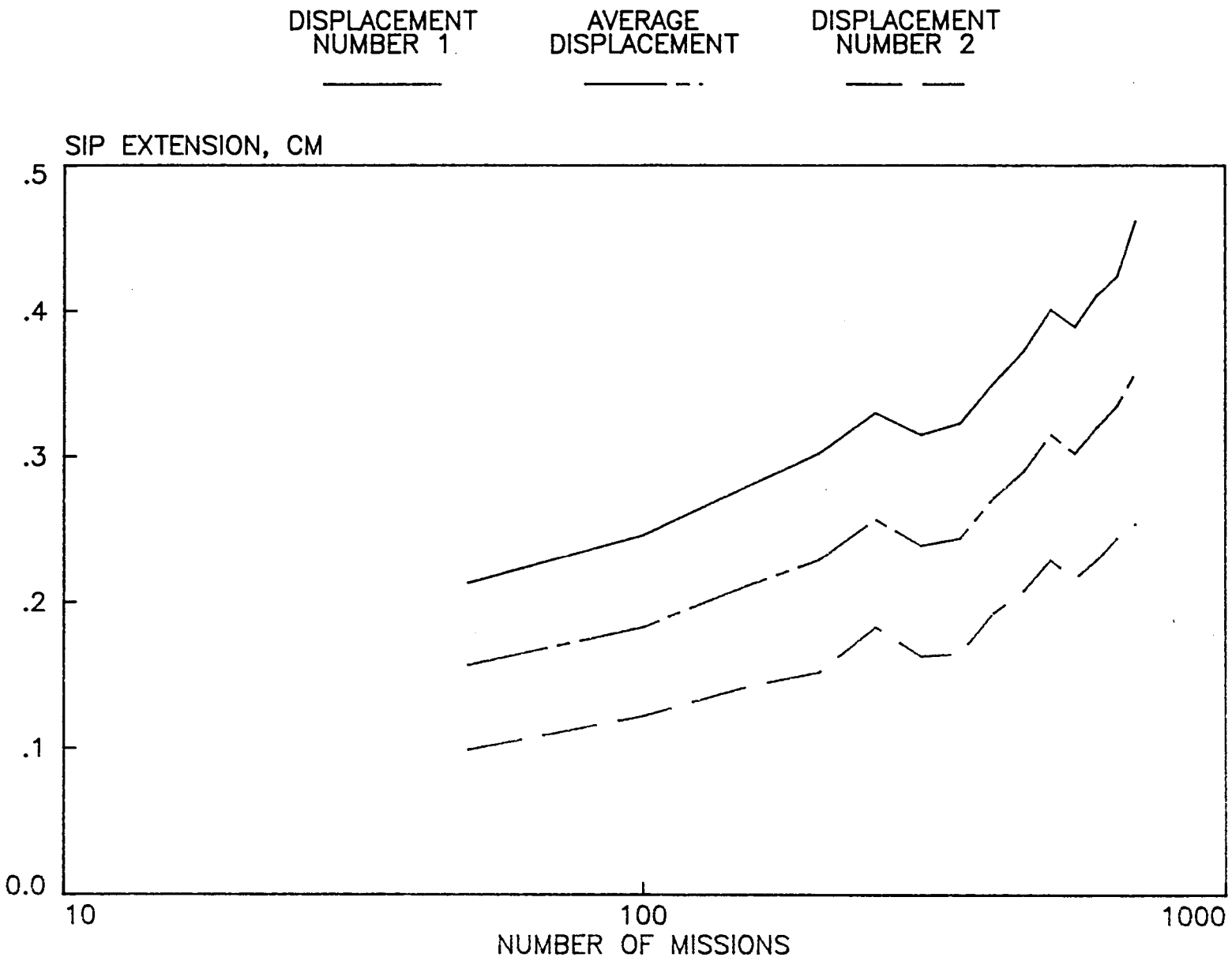

FIGURE 13.- ABSOLUTE SIP EXTENSION FOR TILE FLD-2 AFTER REMOVAL OF STATIC LOAD AS A FUNCTION OF THE NUMBER OF SIMULATED MISSIONS.

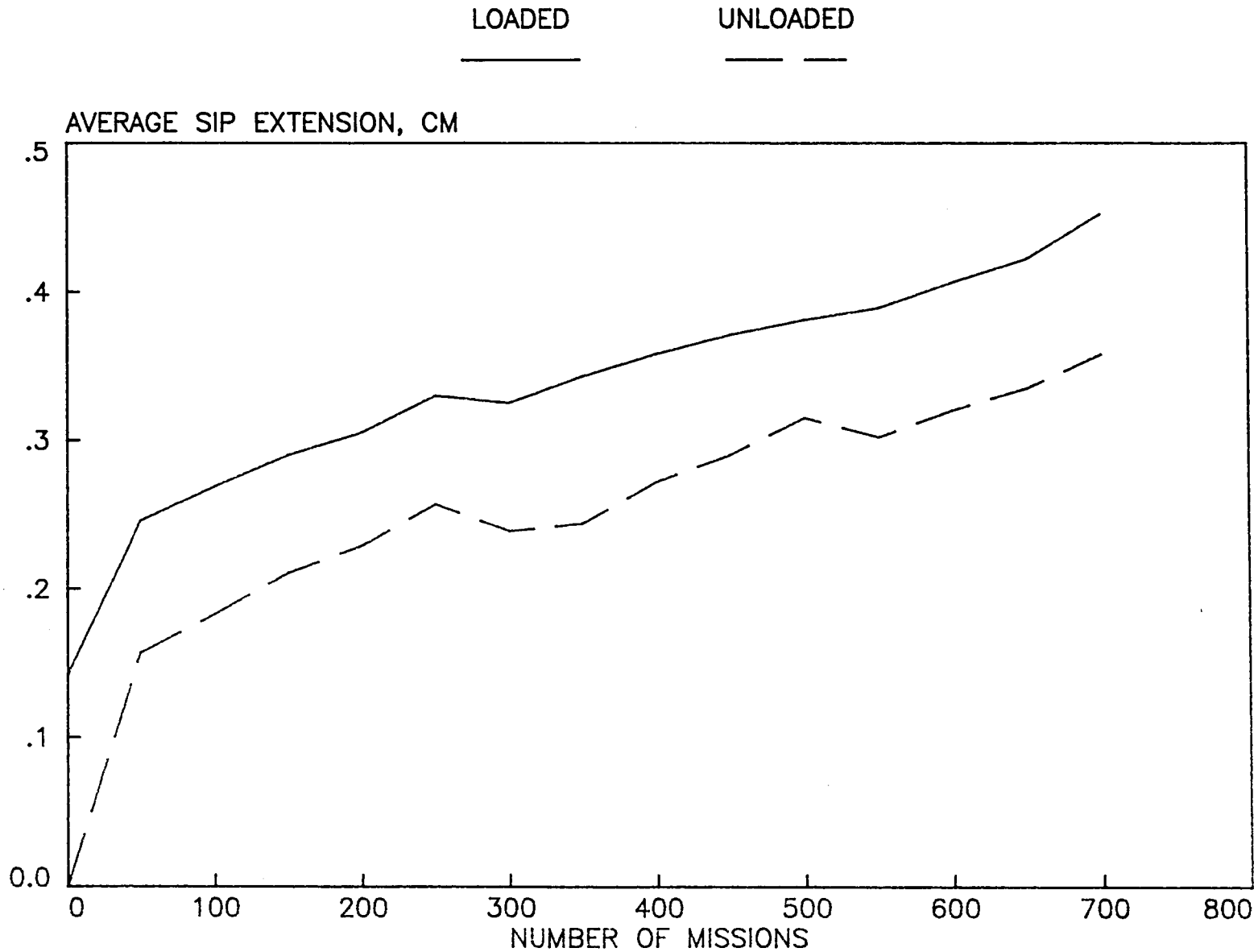

FIGURE 14.- COMPARISON OF LOADED AND UNLOADED AVERAGE SIP EXTENSION FOR TILE FLD-2.

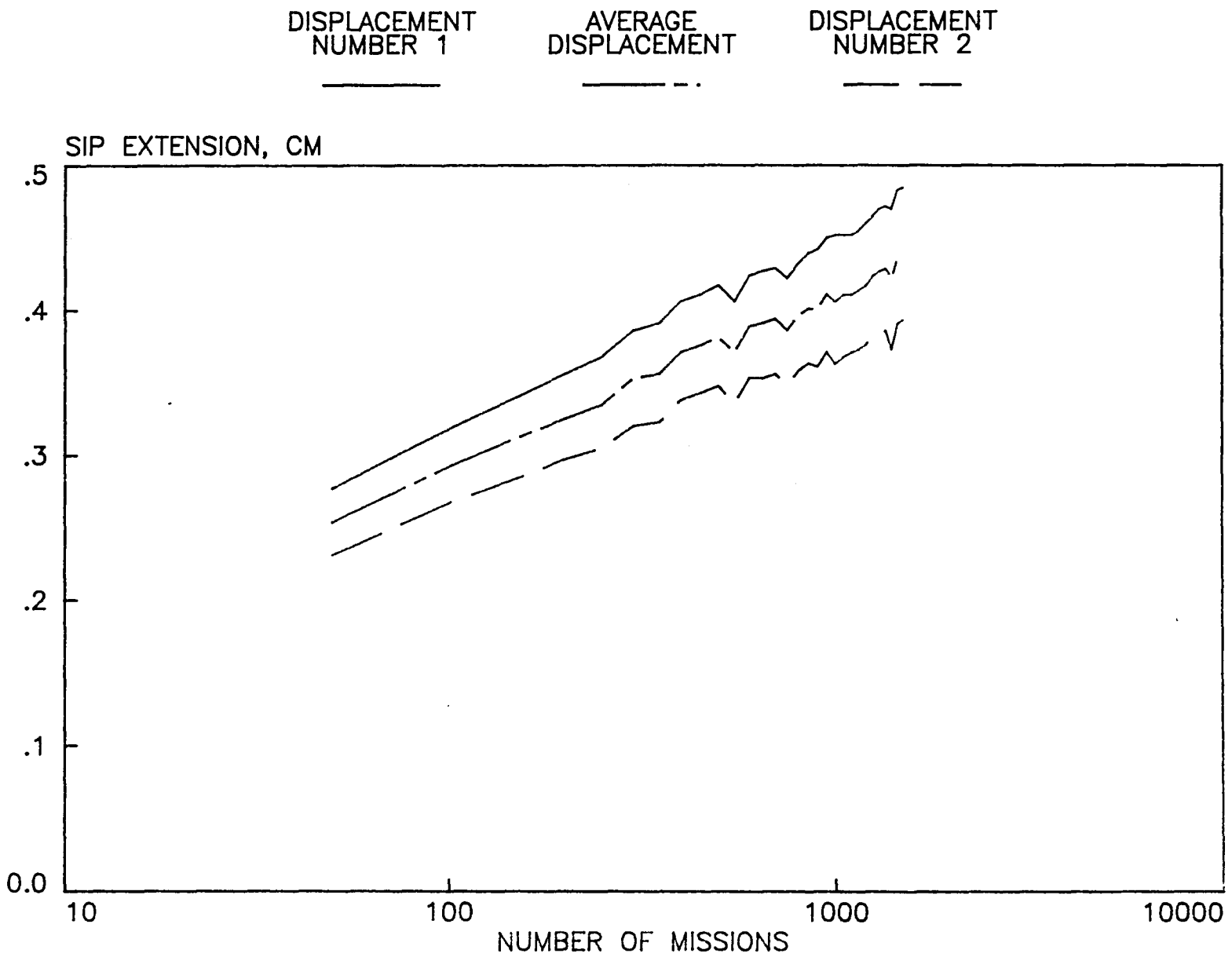

FIGURE 15.- ABSOLUTE SIP EXTENSION FOR TILE FLD-4 AS A FUNCTION OF THE NUMBER OF SIMULATED MISSIONS (STATIC STRESS = 22.4 KPA).

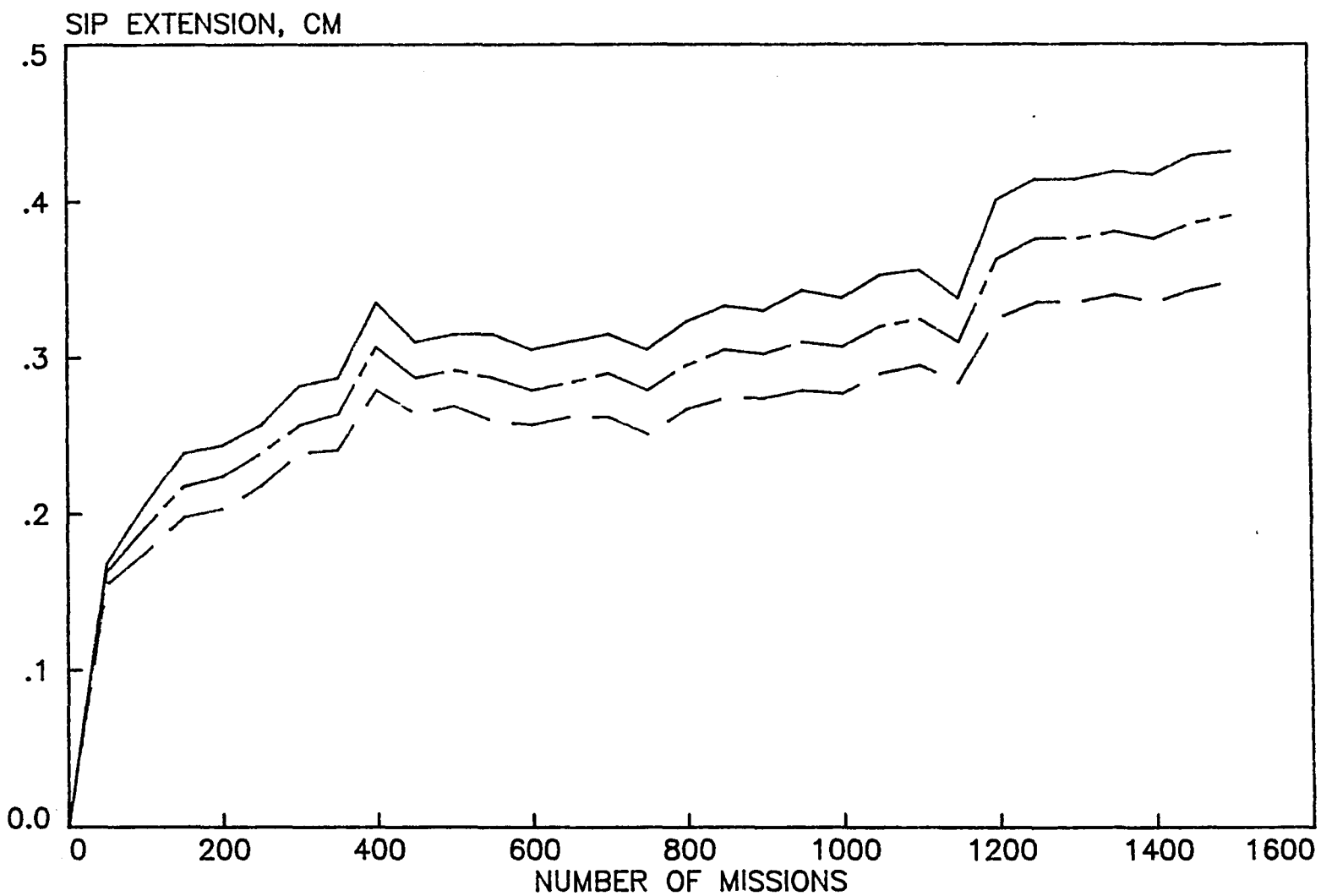

FIGURE 16.- ABSOLUTE SIP EXTENSION FOR TILE FLD-4 AFTER REMOVAL OF STATUC LOAD AS A FUNCTION OF THE NUMBER OF SIMULATED MISSIONS.

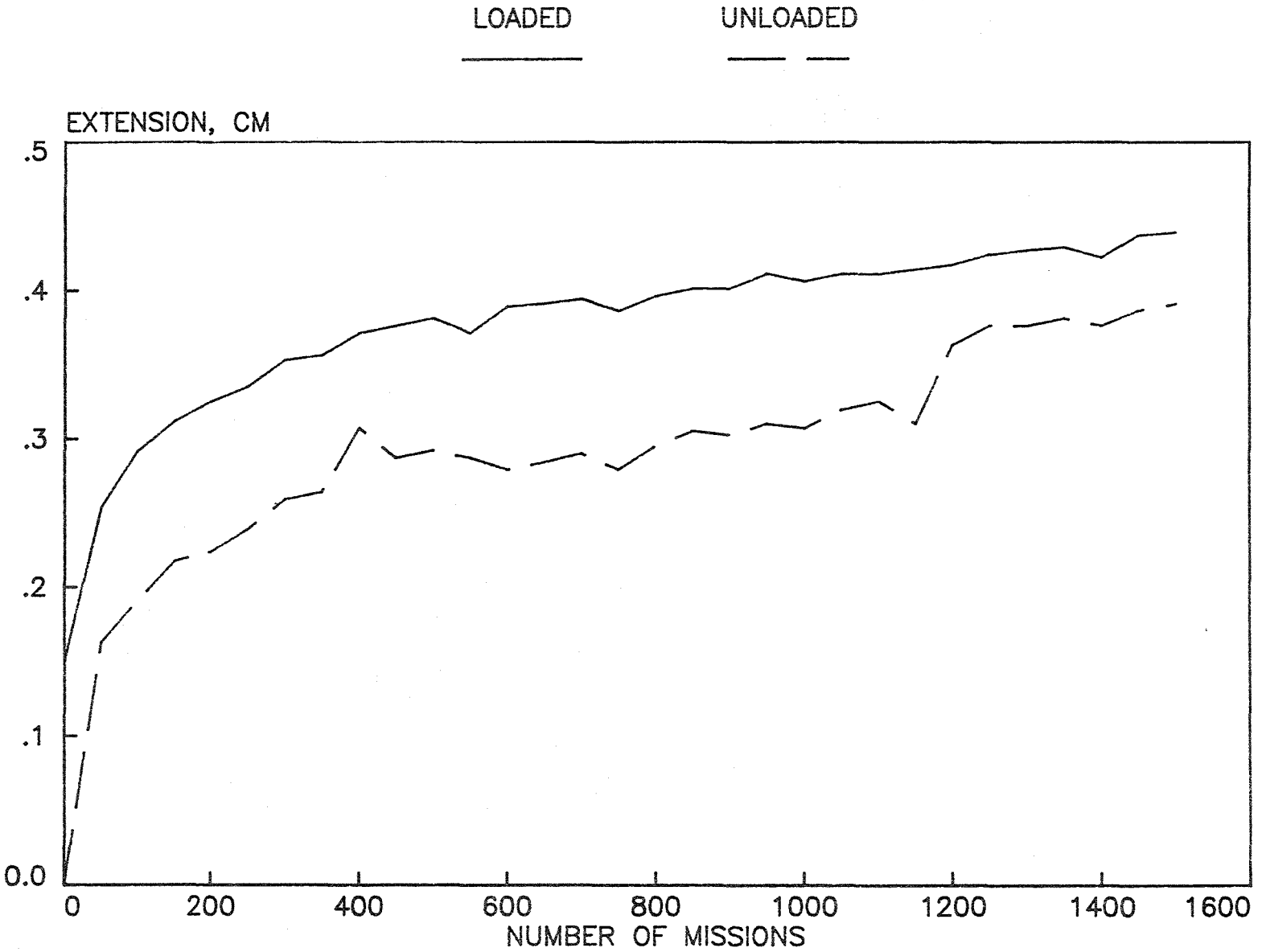

FIGURE 17.- COMPARISON OF LOADED AND UNLOADED AVERAGE SIP EXTENSION FOR TILE FLD-4.

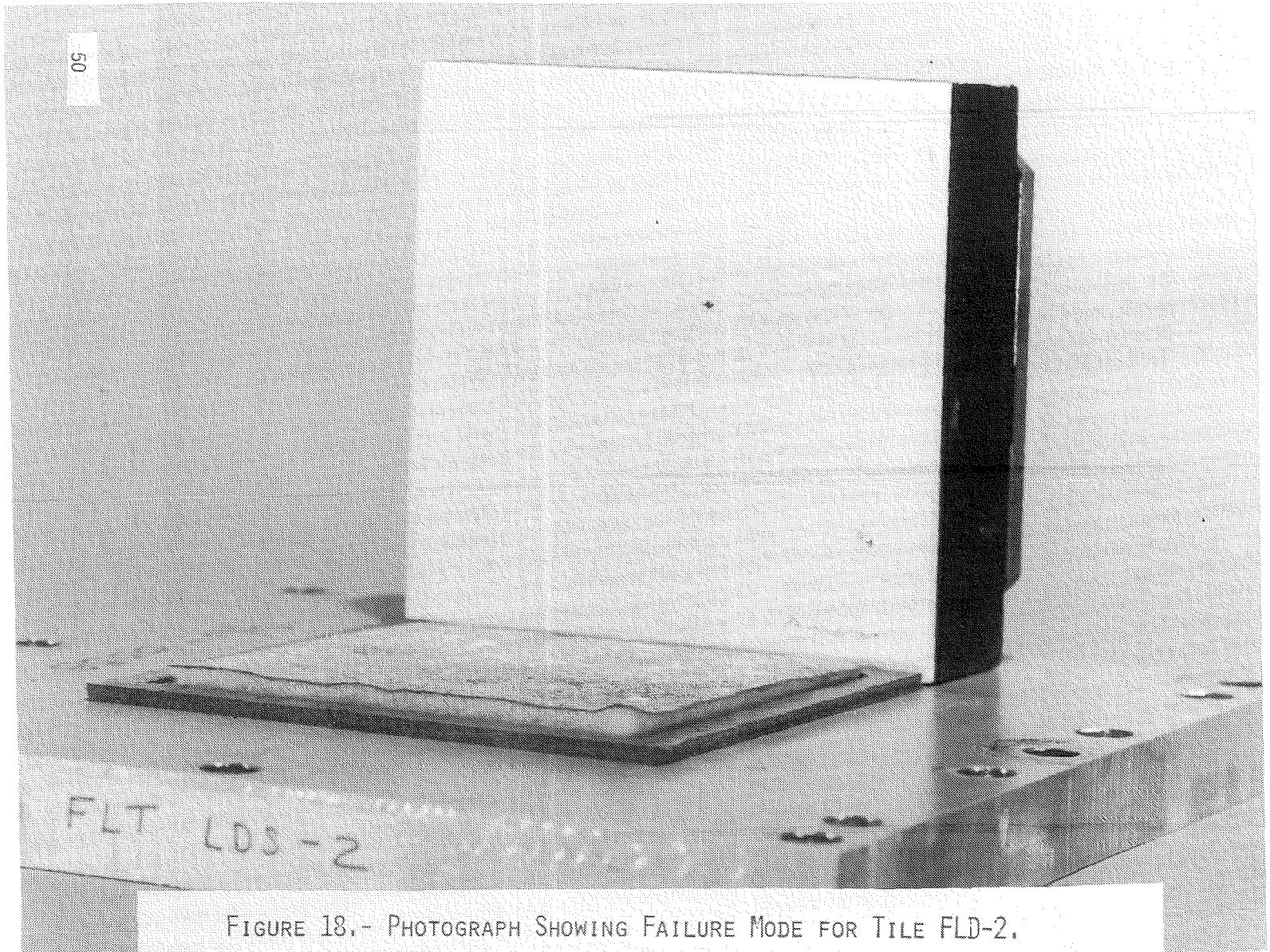

FIGURE 18.- PHOTOGRAPH SHOWING FAILURE MODE FOR TILE FLD-2.

1. Report No.	2. Government Accession No.	3. Recipient's Catalog No.
NASA TM-83148		

4. Title and Subtitle	5. Report Date
Mission Load Dynamic Tests of Two Undensified Space Shuttle Thermal Protection System Tiles	June 1981
	6. Performing Organization Code: 506-89-01-01

7. Author(s)	8. Performing Organization Report No.
Jack D. Leatherwood and Joe C. Gowdey	
	10. Work Unit No.

9. Performing Organization Name and Address	11. Contract or Grant No.
NASA Langley Research Center Hampton, VA 23665	
	13. Type of Report and Period Covered: Technical Memorandum

12. Sponsoring Agency Name and Address	14. Sponsoring Agency Code
National Aeronautics and Space Administration Washington, DC 20546	

15. Supplementary Notes

16. Abstract

Two tests of undensified Space Shuttle thermal protection tiles under combined static and dynamic loads have been conducted. The tiles had a density of approximately 144 Kg/m^3 (LI900 tiles) and were mounted on a strain isolation pad which was 0.41 cm (.160 inch) thick. A combined static and dynamic mission stress histogram representative of the W-3 area of the wing of the orbiter vehicle was applied. The stress histogram was provided by the Space Shuttle Project. Results presented in this paper include: tabulation of measured peak and root-mean-square (RMS) accelerations in both compression and tension; peak SIP stress in compression and tension, peak and RMS amplitude response ratios; lateral to vertical response ratios; response time histories; peak stress distributions (histograms), and SIP extension measured both with and without static tension at various mission times.

17. Key Words (Suggested by Author(s))	18. Distribution Statement
Response, Fatigue, Vibration, Nonlinear	Unclassified-Unlimited Subject Category 39

19. Security Classif. (of this report)	20. Security Classif. (of this page)	21. No. of Pages	22. Price*
Unclassified	Unclassified	51	A04

* For sale by the National Technical Information Service, Springfield, Virginia 22161

End of Document